ARTICLE

Retromer and TBC1D5 maintain late endosomal RAB7 domains to enable amino acid–induced mTORC1 signaling

Arunas Kvainickas[1], Heike Nägele[1], Wenjing Qi[2], Ladislav Dokládal[3], Ana Jimenez-Orgaz[1], Luca Stehl[1], Dipak Gangurde[2], Qian Zhao[2] (ORCID), Zehan Hu[3], Jörn Dengjel[3] (ORCID), Claudio De Virgilio[3] (ORCID), Ralf Baumeister[2], and Florian Steinberg[1] (ORCID)

Retromer is an evolutionarily conserved multiprotein complex that orchestrates the endocytic recycling of integral membrane proteins. Here, we demonstrate that retromer is also required to maintain lysosomal amino acid signaling through mTORC1 across species. Without retromer, amino acids no longer stimulate mTORC1 translocation to the lysosomal membrane, which leads to a loss of mTORC1 activity and increased induction of autophagy. Mechanistically, we show that its effect on mTORC1 activity is not linked to retromer's role in the recycling of transmembrane proteins. Instead, retromer cooperates with the RAB7-GAP TBC1D5 to restrict late endosomal RAB7 into microdomains that are spatially separated from the amino acid–sensing domains. Upon loss of retromer, RAB7 expands into the ragulator-decorated amino acid–sensing domains and interferes with RAG-GTPase and mTORC1 recruitment. Depletion of retromer in *Caenorhabditis elegans* reduces mTORC1 signaling and extends the lifespan of the worms, confirming an evolutionarily conserved and unexpected role for retromer in the regulation of mTORC1 activity and longevity.

Introduction

The retromer complex

The evolutionarily conserved retromer complex is a multiprotein complex consisting of the subunits VPS26, VPS29, and VPS35 that resides on the surface of early and late endosomes (Gallon and Cullen, 2015). While the trimeric retromer complex has no intrinsic membrane-binding capabilities, it associates with GTP-bound, activated Rab7 and various phosphoinositide binding sorting nexins (SNXs), which tether retromer to the endosomal limiting membrane (Rojas et al., 2008; Seaman et al., 2009; Harrison et al., 2014). The retromer subunit VPS35 also recruits the actin polymerizing WASH (Wiskott-Aldrich syndrome protein and SCAR homolog) complex onto endosomes to locally generate branched actin networks (Derivery et al., 2009; Gomez and Billadeau, 2009; Harbour et al., 2010, 2012; Helfer et al., 2013). Retromer, acting in concert with the WASH complex and the retromer-associated SNXs, has been shown to function as a master regulator of endocytic recycling that transports a vast variety of transmembrane proteins from endosomes back to the cell surface (Steinberg et al., 2013) and also to the trans-Golgi network (Arighi et al., 2004; Seaman, 2004; Burd and Cullen, 2014). Besides its well-documented role in the recycling of integral membrane proteins, retromer has also been shown to have noncanonical functions that go beyond endocytic recycling: retromer can shut down signaling receptors at the endosomal level (Feinstein et al., 2011), it has been proposed to function in transport to and from mitochondria (Braschi et al., 2010), and it is likely involved in some forms of autophagy (Zavodszky et al., 2014; Jimenez-Orgaz et al., 2018). In addition, we have recently demonstrated that retromer and the retromer-bound RAB–GTPase-activating protein (GAP) protein TBC1D5 function as master regulators of the late endocytic small GTPase RAB7 (Jimenez-Orgaz et al., 2018). Given these precedents, it is highly likely that retromer has additional, noncanonical functions that remain to be discovered. Importantly, a point mutation in the retromer subunit VPS35 has been identified to cause hereditary Parkinson's disease (Vilariño-Güell et al., 2011; Zimprich et al., 2011), which makes a thorough understanding of all retromer functions relevant from a medical perspective.

[1]Center for Biological Systems Analysis, University of Freiburg, Freiburg, Germany; [2]Faculty of Biology, University of Freiburg, Freiburg, Germany; [3]Department of Biology, University of Fribourg, Fribourg, Switzerland.

Correspondence to Florian Steinberg: florian.steinberg@zbsa.de.

Mechanistic (formerly mammalian) target of rapamycin (mTOR) signaling

mTOR is a serine/threonine kinase that is part of two independent protein complexes termed mTORC1 and mTORC2, which are defined by their distinct subunit composition and their divergent role in cellular signaling (Saxton and Sabatini, 2017). The core of mTORC1 is composed of the mTOR kinase, RAPTOR (regulatory-associated protein of mTOR), and mLST8 (Hara et al., 2002; Kim et al., 2002), while mTORC2 contains mTOR and RICTOR (Sarbassov et al., 2004) as well as mLST8. mTORC2 mainly senses growth factor signaling and promotes cell survival, whereas mTORC1 and its regulatory network is the central nutrient, energy, and growth signal–sensing mechanism of the cell (Saxton and Sabatini, 2017). mTORC1 is activated by nutrient and growth factor abundance and deactivated by a lack of nutrients, most notably amino acids. The presence of amino acids is detected by a complex machinery that localizes to the cytosolic leaflet of the late endosomal/lysosomal membrane. There, amino acid channels, the vesicular proton pump v-ATPase and the pentameric ragulator complex as well as a host of regulatory factors detect amino acids (Sancak et al., 2010; Zoncu et al., 2011; Bar-Peled et al., 2012; Wang et al., 2015; Wolfson and Sabatini, 2017), which leads to activation of RAG GTPase dimers that directly bind to RAPTOR (Sancak et al., 2008). This binding serves to recruit mTORC1 to the lysosome, where it is activated by RHEB (Inoki et al., 2003; Tee et al., 2003; Sancak et al., 2010), another small GTPase that localizes to lysosomes (Menon et al., 2014). When nutrients, energy, and growth factors are abundant, maximally activated mTORC1 phosphorylates substrates such as S6 kinase 1 (S6K1), which in turn phosphorylates downstream substrates that govern translation and cellular growth. In the absence of nutrients, mTORC1 is inactive, its substrates are less phosphorylated, and cellular growth is inhibited. An absence of mTORC1 signaling causes the cell to activate the autophagic self-digestion program to release nutrients from nonessential cellular components. As a central sensor of nutrients and regulator of cellular growth, it is not surprising that deregulated mTOR signaling has been implicated in diseases such as cancer and diabetes (Saxton and Sabatini, 2017).
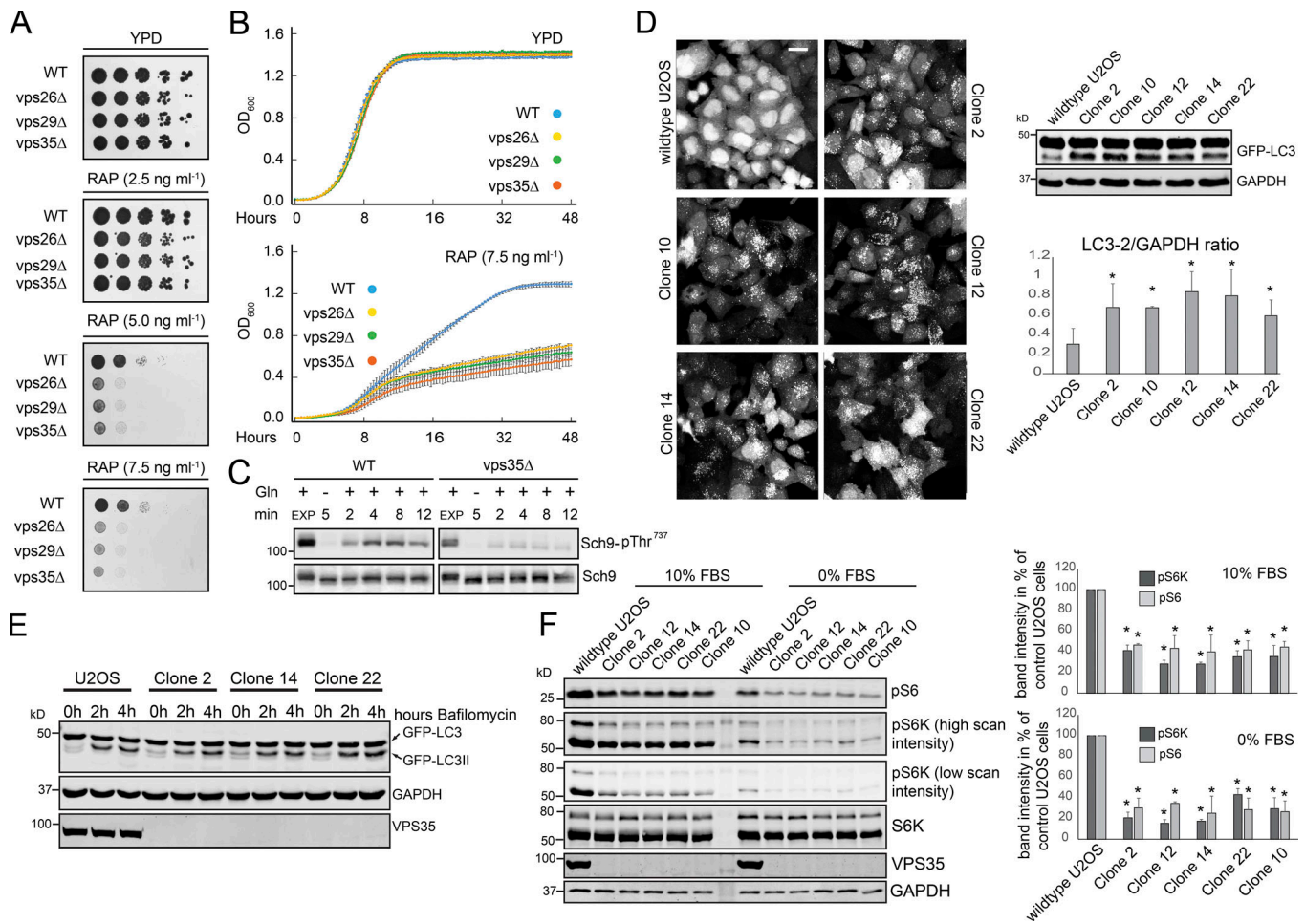
Retromer and mTOR

A large-scale genetic screen for genes modulating sensitivity to the mTORC1 inhibitor rapamycin identified the retromer subunit VPS35 as a modulator of mTORC1 activity (Xie et al., 2005). Loss of VPS35 resulted in increased sensitivity to rapamycin, suggesting that VPS35 could promote mTORC1 activity. Given that retromer is intimately involved in lysosomal homeostasis, a potential connection between retromer and the lysosomally controlled mTORC1 complex appeared conceivable. Here, we establish retromer as an evolutionarily conserved regulator of mTORC1 activity. Mechanistically, retromer cooperates with the RAB7-specific GAP protein TBC1D5 to restrict RAB7 localization and activity to late endosomal microdomains, which enables amino acid sensing at the late endosome/lysosome to promote mTORC1 activity.

Results

Since depletion of VPS35 in yeast resulted in rapamycin hypersensitivity in a large-scale screen (Xie et al., 2005), we aimed to confirm this data in a more targeted manner. Indeed, deletion of each of the essential retromer subunits VPS26, VPS29, and VPS35 in yeast led to rapamycin-sensitive growth inhibition, on plates as well as in liquid cultures (Fig. 1, A and B). Amino acid–induced phosphorylation of the TORC1 substrate Sch9 was also markedly reduced in the VPS35 mutant strain, indicating that retromer-deficient yeast display mTORC1 defects. We next tested whether these defects were conserved in mammalian cells. To do so, we employed previously described VPS35- and VPS29-deficient U2OS osteosarcoma and HeLa cell lines generated with transcription activator-like effector nucleases (TALEN) and CRISPR/Cas9 technology, respectively (Kvainickas et al., 2017a). These cells display a loss of the core retromer trimer from endosomes but retain vesicular SNX1 signal (Fig. S1 A), as these subcomplexes of retromer assemble and function independently (Kvainickas et al., 2017a). The VPS35-deficient U2OS cell lines suffered from growth defects (Fig. S1 B), and residual growth was hypersensitive to treatment with low concentrations of the mTORC1 inhibitor rapamycin (Fig. S1 C). Since retromer has been linked to nutrient uptake as well as to autophagy (Zavodszky et al., 2014; Kvainickas et al., 2017b), we also analyzed the autophagic state of the retromer-deficient cell lines. All of the VPS35-deficient cell lines displayed more vesicular GFP-LC3, corresponding to increased levels of lipidated LC3 (Fig. 1 D). As reported previously for HeLa cells (Zavodszky et al., 2014; Jimenez-Orgaz et al., 2018), the autophagic flux, measured through LC3 turnover in starved cells treated with the lysosome inhibitor bafilomycin, was not perturbed (Fig. 1 E). This indicated that the increase in lipidated LC3 was caused not by impaired lysosomal degradation of autophagosomes but instead by increased de novo induction of autophagy. Consistent with increased rapamycin sensitivity and up-regulated autophagy, the phosphorylation state (T389) of the widely used mTORC1 target S6K and its downstream target ribosomal protein S6 were much lower in the U2OS VPS35 knockout (KO) cell lines in the presence as well as in the absence of serum (Fig. 1 F). The VPS29-deficient HeLa cells also displayed a pronounced loss of phosphorylation across several mTORC1 substrates (Fig. S1 D), confirming the U2OS data (Fig. S1 D). We also found that transcription factor EB (TFEB), which is kept in the cytosol by mTORC1-mediated phosphorylation (Martina et al., 2012; Roczniak-Ferguson et al., 2012; Settembre et al., 2012), was nuclear in VPS35 and VPS29 KO cells (Fig. 2 A), whereas it was cytosolic in parental cells (Fig. 2 A). Taken together, our results indicate that retromer-deficient eukaryotic cells display impaired mTORC1 activity, resulting in higher levels of autophagy induction, TFEB translocation, and proliferation defects.

mTORC1 defects are not caused by generic cell stress, loss of mTORC1, recycling defects, or impaired growth factor signaling

To identify the cause for the apparent mTORC1 defects in retromer-deficient cells, we first tested whether loss of retromer caused generic cellular stress, which has been demonstrated to

Kvainickas et al.
Retromer maintains amino acid signaling

Journal of Cell Biology 3020
https://doi.org/10.1083/jcb.201812110

Figure 1. Loss of retromer causes mTORC1 activity defects in *S. cerevisiae* and mammalian cells. (A) WT and retromer complex mutants *vps26Δ*, *vps29Δ*, and *vps35Δ* were grown to exponential growth phase, spotted (10-fold serial dilutions) on YPD plates containing no (YPD only) or the indicated concentrations of rapamycin, and grown for 3 d at 30°C. **(B)** Strains (as in A) were inoculated in liquid YPD (top panel) or YPD containing 7.5 ng ml^{-1} rapamycin (lower panel), and growth was monitored using a Bioscreen C reader set at 30°C with readings (OD$_{600}$) taken every 30 min. **(C)** Strains (as in A) were grown exponentially in synthetic complete medium (+; EXP), starved for amino acids for 5 min (−; 5 min) and restimulated with 3 mM glutamine for the indicated times (+ Gln; 4–12 min). Phosphorylation of the TORC1 target residue Thr^{737} within Sch9 (Urban et al., 2007) was monitored by immunoblot analysis using anti-Sch9-pThr^{737} and anti-Sch9 antibodies. **(D)** Parental U2OS and VPS35 KO cells infected with a lentivirus expressing GFP-LC3 were cultured in full growth medium and fixed in PFA followed by confocal microscopy of the GFP-tag. The same cells were also lysed, and lipidation of LC3b was tested by Western blotting. The quantification was done across three independent experiments. **(E)** Autophagic flux in three VPS35-deficient cell lines and parental U2OS cells was analyzed by Western blotting of GFP-LC3B in lysates from EBSS-starved and Bafilomycin A1–treated cells. **(F)** Parental U2OS cells and the indicated VPS35 KO cell lines were cultured in the presence (left) and absence (right) of FBS, and mTORC1 activity was assayed by Western blotting of phosphorylated S6K1 (and phospho-S6 as a further control of S6K1 activity). The quantifications were done across three independent experiments. Error bars = SD. Scale bars represent 10 μm; *, P < 0.05 in a two-tailed, unpaired *t* test between the indicated condition and parental/nontreated control cells.

lead to lysosomal recruitment of the mTORC1 deactivating GAP protein complex TSC1/2 (Demetriades et al., 2016). This complex is recruited to lysosomes by generic cellular stress, where it deactivates the mTORC1 activating small GTPase RHEB (Garami et al., 2003), thereby shutting off mTORC1 activity. However, endogenous tuberous sclerosis complex 2 (TSC2) was cytosolic in the VPS35 KO clones (Fig. 2 B), comparable to the distribution in parental U2OS cells. We also tested whether the early and late endocytic network remained separated, which is known to be a requirement for amino acid sensing (Flinn et al., 2010). The early endosomal markers EEA1 and SNX1 remained well separated from the late endocytic marker LAMP1 (Fig. S1 E), indicating that loss of retromer does not cause a merging of the early

and late endocytic compartment. Since retromer is an endocytic trafficking complex, we also tested whether the lysosomal arginine sensor and mTORC1 activator SLC38A9 (Jung et al., 2015; Rebsamen et al., 2015; Wang et al., 2015), an integral membrane protein, was correctly positioned in retromer-deficient cells. FLAG-tagged SLC38A9 was correctly positioned relative to LAMP1-decorated lysosomes (Fig. 2 C) and to the ragulator complex (Fig. S1 F), with which SLC38A9 interacts to activate mTORC1 on lysosomes (Shen and Sabatini, 2018). We also tested whether mTORC1 was normally present and correctly assembled in the VPS35 KO cells through precipitation of lentivirally expressed GFP-MLST8, which is a component of both mTORC1 and mTORC2 (Kim et al., 2003; Jacinto et al., 2004). As shown in
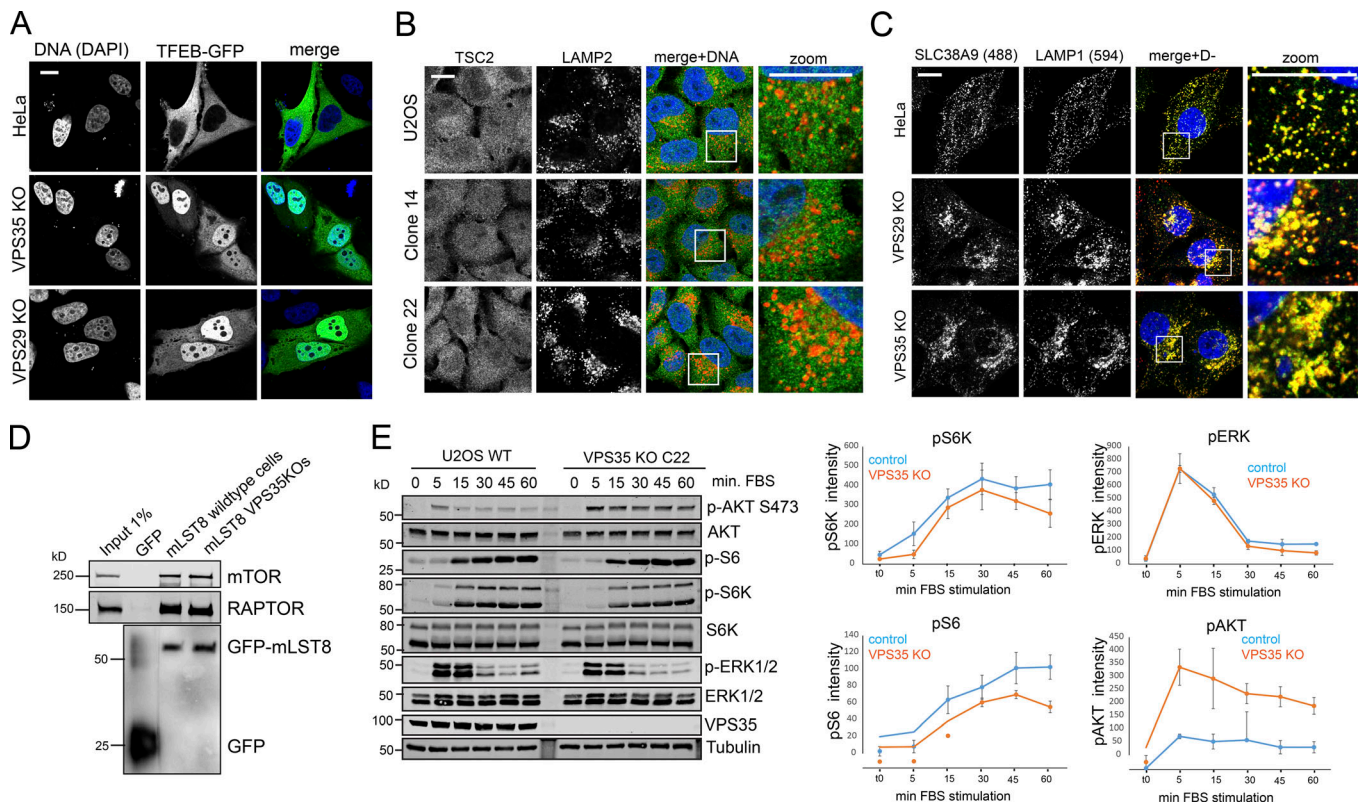
Figure 2. **mTORC1 regulation through growth factors, TSC2, and SLC38A9 localization in retromer-deficient cells. (A)** TFEB-GFP was transiently expressed in parental HeLa cells and in VPS35 and VPS29 KO cells. Parental and clonal VPS35 deficient U2OS cells were serum starved overnight and treated with dialyzed FBS for the indicated time points. Activation of mTORC1 was tested through Western blotting of phosphorylated mTORC1 substrates S6K1 and S6. **(B)** Parental U2OS and two clonal VPS35 KO cell lines were fixed and stained for endogenous TSC2 (Alexa Fluor 488, green) and LAMP2 (Alexa Fluor 594, red). **(C)** FLAG-SLC38A9 (Alexa Fluor 488, green) was lentivirally expressed in parental and VPS29 or VPS35 KO HeLa cells and costained with the lysosome marker LAMP1 (Alexa Fluor 594, red). **(D)** GFP-mLST8 was lentivirally expressed in WT and VPS35-deficient cells and precipitated through GFP-trap beads. The precipitates were analyzed for mTORC1 assembly by Western blotting for endogenous RAPTOR and mTOR. **(E)** Parental and VPS35 KO U2OS cells were serum starved overnight and stimulated with dialyzed FBS for the indicated times. mTORC1 substrate phosphorylation was assessed through Western blotting. Quantifications were done across three independent experiments. Scale bars represent 10 µm. Error bars = SD.

Fig. 2 D, GFP-mLST8 precipitated endogenous mTOR and RAPTOR normally from VPS35 KOs, indicating unperturbed formation of mTORC1 in the absence of retromer. Collectively, these data argued for a more specific defect in mTORC1 activation.

As mTORC1 can be activated by growth factor signaling as well as by nutrient and energy availability, we next sought to determine which of these mTORC1 stimuli might be affected by loss of VPS35. The decrease of mTORC1 substrate phosphorylation in serum-starved cells (Fig. 1 F) argued against a defect in growth factor signaling as the underlying cause. Indeed, extensive serum (growth factor) stimulation experiments with dialyzed FBS (to avoid changes in amino acid composition of the medium) revealed that growth factor signaling was almost unperturbed in cells treated with a highly efficient siRNA against VPS35 as well as in the KO clones (Figs. 2 E and S2, A and B). Similarly, EGF normally activated mTORC1 substrate phosphorylation in the VPS29-deficient HeLa cell line (Fig. S2 C). Interestingly, activation of AKT (S473), an mTORC2 target site (Sarbassov et al., 2005), was strongly increased in knockdown and KO cells, while activation of ERK1/2 was unperturbed compared with control cells (Figs. 2 E and S2, A–C). These data

argued that growth factor–mediated activation of mTORC1 is not negatively affected by loss of retromer.

Amino acids signaling is perturbed upon loss of retromer

In stark contrast, acute stimulation of nutrient-starved cells with amino acids revealed dramatically reduced phosphorylation of the mTORC1 substrates S6K and S6 in all tested U2OS VPS35 KO cell lines compared with parental cells (Fig. 3 A). Readdition of amino acids for 45 min after 3 h of starvation also led to reduced mTORC1 substrate phosphorylation in U2OS cells treated with siRNA against VPS35 (Fig. 3 B). Time course experiments with amino acid reexposure from 5 to 60 min (Fig. 3, C and D) and up to 3 h (Fig. S2 D) with VPS35 knockdown and KO cells revealed lower mTORC1 substrate phosphorylation across all time intervals. mTORC1 is known to change its subcellular localization in an activity-dependent manner: in nutrient deprived cells, inactive mTORC1 is mainly cytosolic but relocalizes to lysosomes in response to nutrient (amino acid) availability (Sancak et al., 2010). Dual imaging of lysosomes and of the endogenous mTOR kinase revealed that mTOR failed to relocalize to lysosomes in response to amino acid stimulation in VPS35 KO (Fig. 3 E) and VPS35 knockdown (Fig. S2 E) cell lines, thereby
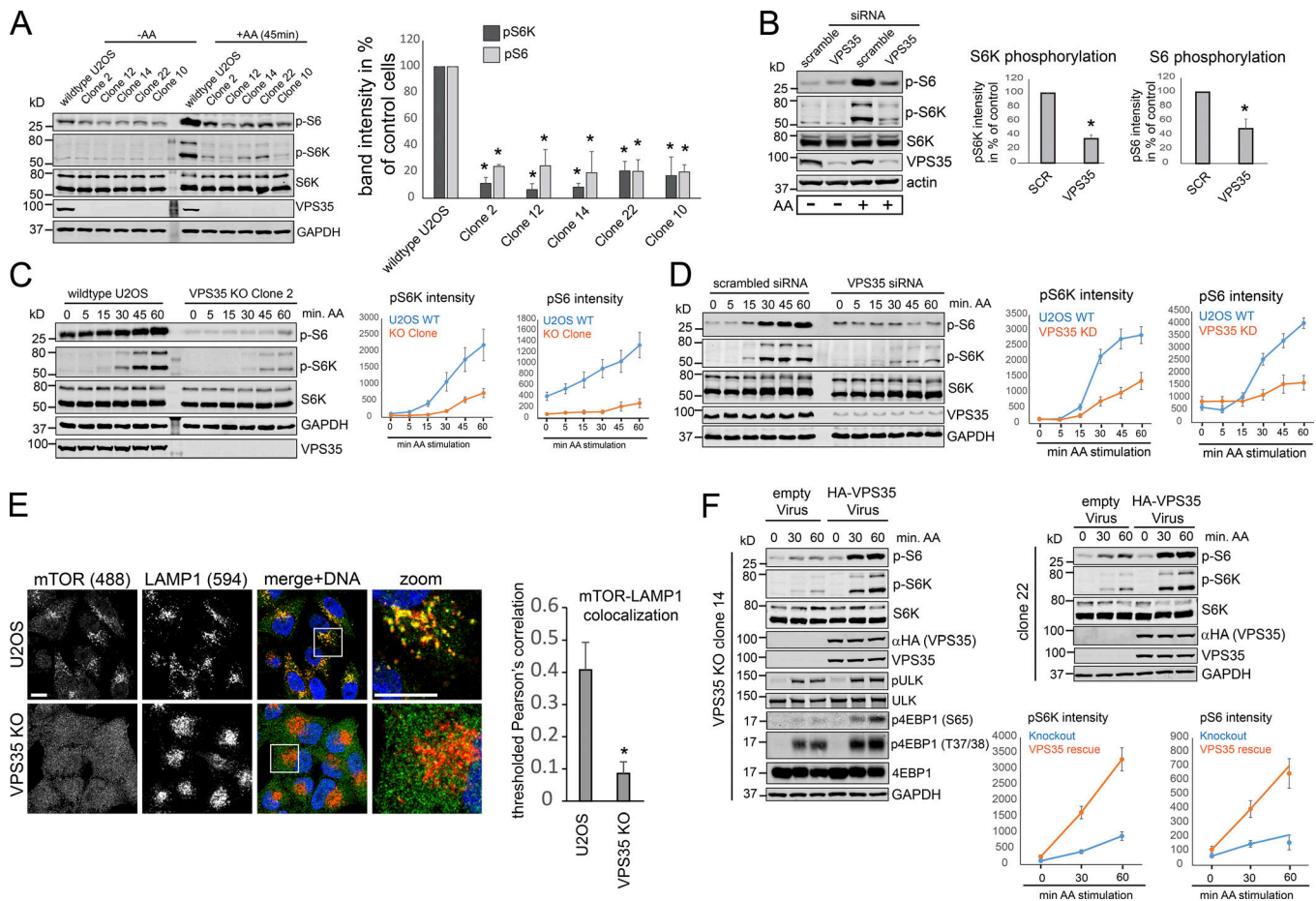
Figure 3. **Loss of VPS35 perturbs amino acid signaling and mTOR recruitment in U2OS osteosarcoma cells. (A)** Parental U2OS cells and five clonal VPS35 KO cell lines were starved in EBSS supplemented with glucose and stimulated with amino acids (serum-free DMEM) for 45 min. mTORC1 activation was assessed by Western blotting of phosphorylated mTORC1 substrates S6K1 and S6. The quantification was performed across three independent experiments. **(B)** The experiment described in A was performed with cells that had been treated with siRNA against VPS35. The quantification was done over three independent experiments. **(C)** Parental U2OS cells and a clonal VPS35 KO cell line were starved in EBSS and stimulated with serum-free DMEM for the indicated time points. mTORC1 activation was assayed by Western blotting of phosphorylated mTORC1 substrates S6K1 and S6. The quantification was done over three independent experiments. **(D)** The experiment described in C was performed in cells treated with siRNA against VPS35 ($n = 3$). **(E)** Parental U2OS cells and a clonal VPS35 KO cell line were starved in EBSS and stimulated with serum free DMEM for 45 min. The cells were fixed in cold PFA and stained for endogenous mTOR (Alexa Fluor 594, red) and LAMP1 (Alexa Fluor 488, green) and DNA (DAPI, blue). The quantification was done across 20 images from two independent experiments. **(F)** Two clonal VPS35 KO cell lines were infected with a lentivirus encoding only puromycin resistance (empty control virus expressing puromycin resistance only) and with a lentivirus encoding HA-VPS35. These cells were then starved in EBSS and stimulated with serum-free DMEM for the indicated times. mTORC1 activation was assessed by Western blotting of phosphorylated mTORC1 substrates. The quantifications were done over three independent experiments. Error bars = SD. Scale bars represent 10 μm; *, $P < 0.05$ in a two-tailed, unpaired t test between the indicated condition and parental/nontreated control cells.

demonstrating that the amino acid stimulation failed to recruit mTOR to the lysosomal membrane in VPS35-deficient cell lines. To exclude clonal or siRNA artifacts, we also used lentiviral reexpression of HA-VPS35 to revert the observed phenotypes. As shown in Fig. 3 F, the loss of mTORC1 substrate phosphorylation in amino acid–stimulated cells could be reverted by reexpression of VPS35 in all clonal U2OS KO cells tested. We also obtained similar results with siRNA-resistant HA-VPS35 in siRNA-treated cells (Fig. S3 A).

To substantiate our data on retromer- and mTORC1-mediated amino acid signaling, we also stimulated retromer-deficient HeLa cells with amino acids. Four independent VPS35 KO clones, described previously (Kvainickas et al., 2017a), displayed lower levels of mTORC1 substrate phosphorylation in full

growth medium (Fig. 4 A). We also detected far lower pS6K and pS6 levels in a clonal VPS29 KO cell line, which could be reverted by lentiviral reexpression of VPS29 (Fig. 4, B and C). Acute stimulation with amino acids across several time points also failed to activate mTORC1 substrate phosphorylation in VPS29 KO cells (Fig. 4 D). We also tested individual amino acids and found that only a combination of leucine and glutamine, as had been reported previously for HeLa cells (Nicklin et al., 2009), efficiently activated mTORC1. The leucine/glutamine-mediated activation of mTORC1 was strongly reduced in the VPS29 KO cells (Fig. 4 E). As had been recently reported for VPS35-deficient HeLa cells (Cui et al., 2019), endogenous mTOR failed to relocalize to LAMP2-decorated lysosomes in amino acid–stimulated VPS29 KO HeLa cells (Fig. 4 F). We could not observe
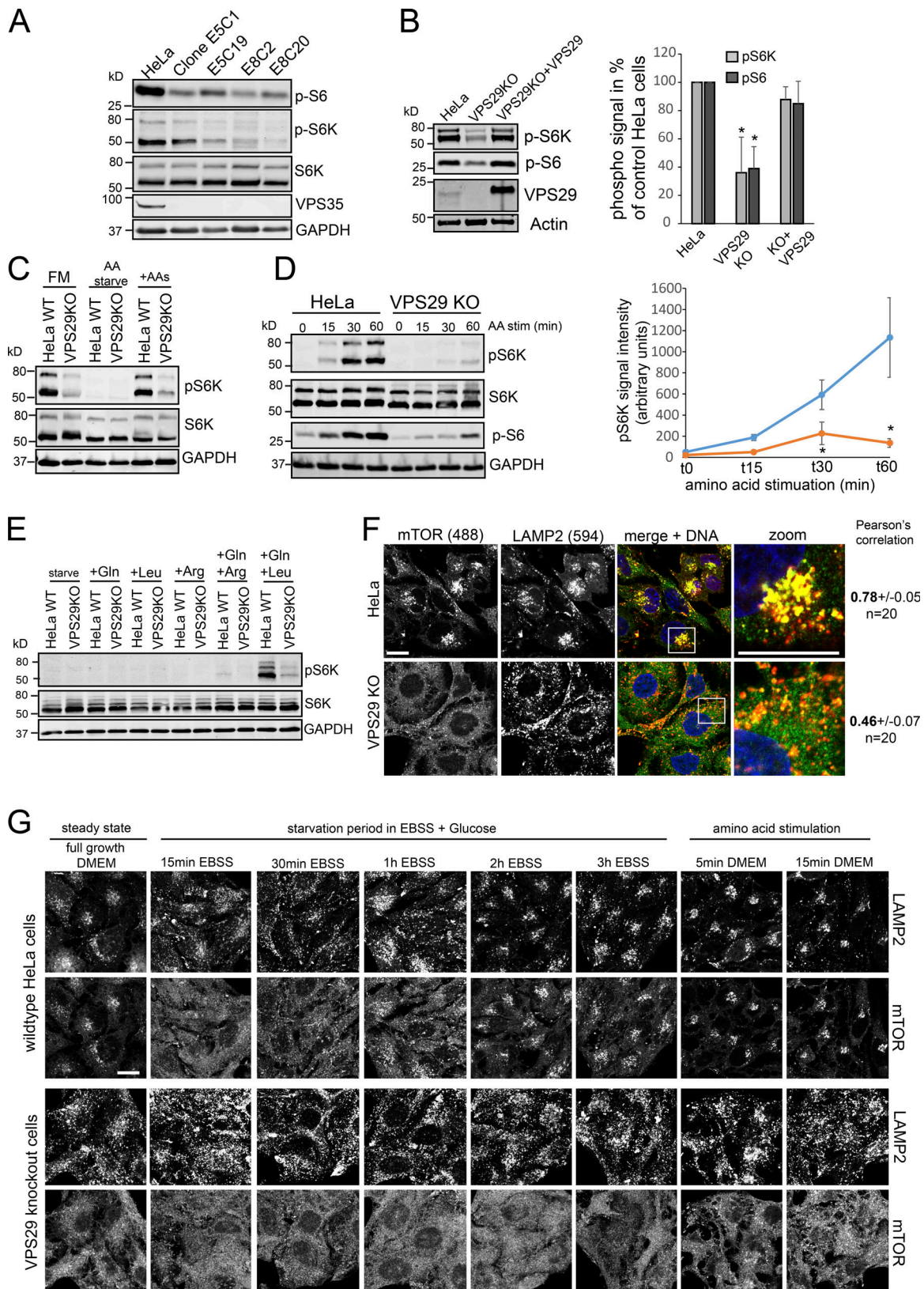
Figure 4. **Amino acid signaling and mTOR recruitment to lysosomes are defective in VPS29-deficient HeLa cells. (A)** Parental HeLa and four VPS35 KO cell lines generated with CRISPR/Cas9 were starved in serum-free DMEM without amino acids and stimulated with a mixture of amino acids (MEM recipe) and glutamine for 45 min. mTORC1 activation was assessed by Western blotting of phosphorylated mTORC1 substrates S6K1 and S6. **(B)** Parental HeLa cells, VPS29 KO cells, and VPS29 KO cells with lentivirally reexpressed VPS29-myc were starved in serum- and amino acid–free medium and stimulated with amino acids for 45 min. The quantification was done over three independent experiments. **(C)** Parental HeLa cells and clonal VPS29 KO cells were cultured in either full growth

medium (FM) or serum- and amino acid–free DMEM (AA starve) or were acutely stimulated with amino acids after 1 h of starvation. mTORC1 activation was assessed by Western blotting of phosphorylated mTORC1 substrates S6K1. **(D)** Parental HeLa cells and VPS29 KO cells were starved in serum- and amino acid–free DMEM and stimulated with amino acids for the indicated time points. mTORC1 activation was assessed by Western blotting of phosphorylated mTORC1 substrates S6K1 and S6. The quantification was done over three independent experiments. **(E)** Parental HeLa cells and VPS29 KO cells were starved in serum- and amino acid–free DMEM and stimulated with the indicated individual amino acids. mTORC1 activation was assessed by Western blotting of phosphorylated mTORC1 substrate S6K1. **(F)** Parental HeLa cells and clonal VPS29 KO cells were starved in serum- and amino acid–free DMEM for 3 h and stimulated with amino acids for 45 min. Following stimulation, cells were fixed and stained for endogenous mTOR (Alexa Fluor 488, green) and endogenous LAMP2 (Alexa Fluor 594, red) and DNA (DAPI, blue). The colocalization between mTOR and LAMP2 was quantified across 20 images from two independent experiments. **(G)** Parental HeLa cells (top panel) and VPS29 KO cells (bottom panel) were starved in EBSS for the indicated time points and stimulated with amino acids for 5 and 15 min. The cells were then fixed in PFA and stained for endogenous mTOR (lower row) and endogenous LAMP2 (upper row). Error bars = SD. Scale bars represent 10 µm; *, P < 0.05 in a two-tailed, unpaired *t* test between the indicated condition and parental/nontreated control cells.

meaningful changes in TSC2 localization in amino acid–starved and stimulated conditions between parental HeLa cells and clonal VPS29 KO cells (Fig. S3 B). Interestingly, we also observed lysosome positioning defects in these cells, as the LAMP2-decorated vesicles failed to cluster in a juxtanuclear area in the KO cells (Fig. 4 F). To substantiate this, we starved these cells for several time points up to 3 h, followed by amino acid stimulation for 5 and 15 min. In parental HeLa cells, lysosomes first moved to the cell periphery upon starvation, followed by previously observed (Korolchuk et al., 2011) progressive clustering in the vicinity of the nucleus. As has been reported previously (Yu et al., 2010), prolonged starvation led to mTOR recruitment to the clustered lysosomes starting at 1 h of starvation (Fig. 4 G). In contrast, lysosomes remained evenly distributed throughout the cytosol at all time points in the VPS29 KO cell line, and mTOR failed to localize to lysosomes during prolonged starvation and also in the amino acid–stimulated cells. In the HeLa cells, we also tested whether the effect on amino acid signaling was specific for retromer. Deletion of the retromer cargo adapter SNX27 (Temkin et al., 2011) and also of the retromer-related retriever complex and SNX17 (McNally et al., 2017) did not result in a reduction of amino acid–mediated mTORC1 activation (Fig. S3 C), suggesting that it is not endocytic recycling in general that is required for mTORC1 activation. We concluded that lysosomal recruitment and activation of mTOR by amino acids was severely perturbed in retromer-deficient cells. This defect appeared to be accompanied by changes in lysosome positioning.

Since mTORC1 is activated by the lysosomal ragulator complex, which acts as a GEF for the RAPTOR binding RAG GTPases (Sancak et al., 2010; Bar-Peled et al., 2012), we next aimed to investigate RAG localization in retromer-deficient cells. The presence of amino acids activates the small GTPases RAGA and RAGB (resulting in RAGA/B-GTP in dimers with inactive RAGC/D-GDP) through a complex regulatory network consisting of the pentameric ragulator complex, amino acid channels, the v-ATPase proton pump, and the GATOR complexes with GAP activity toward the RAGs (Saxton and Sabatini, 2017). Activated RAGA directly binds the mTORC1 subunit Raptor, which is needed for the lysosomal recruitment of mTORC1 and its activation (Sancak et al., 2008, 2010). In agreement with a defect in amino acid signaling, we observed a pronounced loss of the interaction between GFP-RAGA or GFP-RAGB with the endogenous mTORC1 subunit RAPTOR (Fig. 5 A). We also detected a loss of lysosome-localized endogenous RAGC (Fig. 5, B and C) and RAGA (Fig. S3 D) in retromer-deficient HeLa cells, in fed as well

as in starved cells. In agreement with these localization defects, less RAGA and RAGC precipitated with lentivirally expressed LAMTOR1-GFP under fed and starved conditions from VPS35-deficient cells (Fig. 5 D). As reported previously, amino acid stimulation led to a dispersal of the RAGs into the cytosol and weakened the RAG–ragulator interaction (Lawrence et al., 2018). These changes were not caused by ragulator assembly defects, as LAMTOR1-GFP precipitated endogenous LAMTOR2 and LAMTOR4 normally (Fig. 5 D). Precipitation of endogenous LAMTOR1 also coprecipitated similar amounts of endogenous LAMTOR4 from VPS35 KO cells (Fig. 5 E). Furthermore, LAMTOR1-GFP and endogenous LAMTOR4 localized normally to LAMP1-decorated lysosomes (Fig. S3, E and F), indicating unperturbed ragulator assembly and localization. RAG dimerization also appeared to be intact, as isolation of GFP-RAGC from retromer-deficient cells precipitated similar amounts of endogenous RAGA to WT cells (Fig. S3 G). Lentiviral expression of constitutively active RAGA mutants in the retromer-deficient HeLa and U2OS cell lines did not rescue the amino acid signaling defects (Fig. 5, F and G; and Fig. S3 H), suggesting that it is not only RAG activation that is perturbed upon loss of retromer. In agreement with this, KO of the RAG-deactivating GATOR1 GAP complex components NPRL2 and DEPDC5 (Bar-Peled et al., 2013) only modestly increased amino acid–mediated mTORC1 substrate phosphorylation. Overall, our data indicated that RAG recruitment to lysosomes was perturbed upon loss of retromer.

Retromer indirectly regulates mTORC1

Next, we aimed to investigate the mechanistic basis of the apparent role of retromer in the maintenance of amino acid signaling. Since retromer is involved in the recycling of potentially hundreds of different cell surface proteins, we first investigated whether retromer is needed to maintain the cell surface levels of one or several of the critical amino acid transporters that transport the amino acids needed for mTORC1 activation. To this end, we labeled U2OS cells in stable isotope labeling with amino acids in cell culture (SILAC) medium, depleted VPS35 by siRNA, and isolated the cell surface proteome through biotinylation with a cell-impermeable biotin tag. Following streptavidin-based isolation of the biotinylated cell surface proteins, samples from control and VPS35-depleted cells were combined and quantified by liquid chromatography/tandem mass spectrometry (LC-MS/MS; Fig. 6 A). This analysis revealed that all detected amino acid transporters with reported functions in mTOR activation (Nicklin et al., 2009; Heublein et al., 2010; Karunakaran
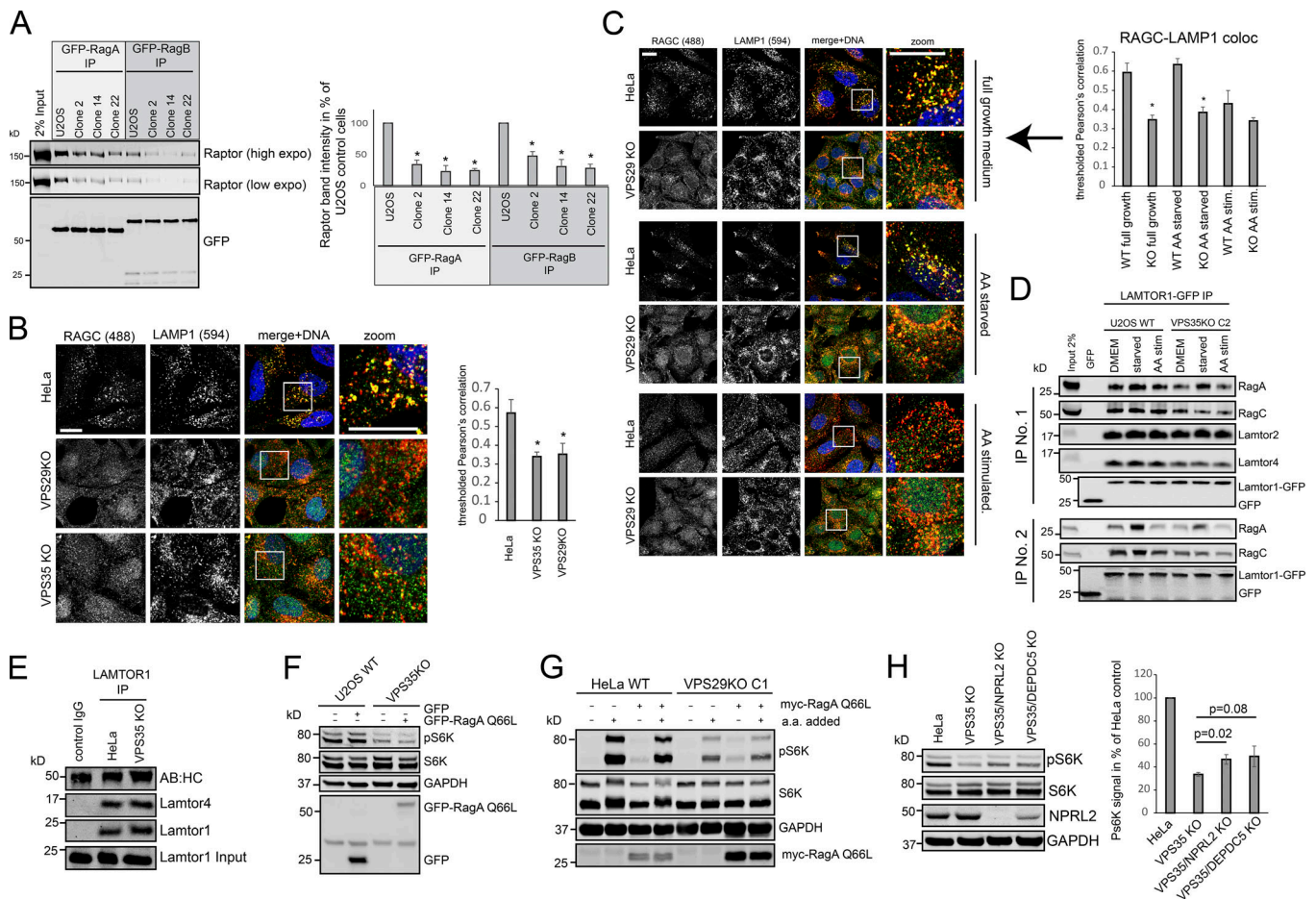
Figure 5. **Loss of retromer perturbs lysosomal recruitment of RAG GTPases. (A)** GFP-RAGA and GFP-RAGB were lentivirally expressed in parental and VPS35-deficient U2OS cells and precipitated with GFP-trap beads. The precipitates were then analyzed for the presence of endogenous Raptor to assess the extent of RAG-Raptor binding (n = 3). **(B)** Endogenous RAGC (Alexa Fluor 488, green) and endogenous LAMP1 (Alexa Fluor 594, red) were costained in parental and in retromer-deficient HeLa cells, and colocalization was analyzed across 20 images from two independent experiments. **(C)** Endogenous RAGC (Alexa Fluor 488, green) and endogenous LAMP1 (Alexa Fluor 594, red) were costained in fed, starved, and amino acid–stimulated (30 min) HeLa cells, and colocalization was analyzed across 20 images from two independent experiments. **(D)** LAMTOR1-GFP was lentivirally expressed in the indicated cell lines, the cells were starved and stimulated, and LAMTOR1-GFP was precipitated by GFP-Trap. Precipitates were analyzed for the presence of RAGs and ragulator components. **(E)** Endogenous LAMTOR1 was precipitated from the indicated HeLa cell lines, and the precipitates were analyzed for the presence of LAMTOR4. **(F and G)** The indicated U2OS and HeLa cells were infected with lentiviruses encoding constitutively active GFP-RAGA-Q66L or myc-tagged RAGA-Q66L, starved in amino acid–free DMEM, and stimulated with amino acids followed by assessment of mTORC1 substrate phosphorylation **(H)** Parental HeLa cells, VPS29 KO cells, and VPS29/NPRL2 or VPS29/DEPDC5 double-KO cells were starved and stimulated with amino acids, and mTORC1 substrate phosphorylation was assessed. Phosphorylated S6K1 signal was quantified across four independent experiments. Error bars = SD. Scale bars represent 10 μm; *, P < 0.05 in a two-tailed, unpaired t test between the indicated condition and parental/nontreated control cells.

et al., 2011; Ögmundsdóttir et al., 2012; Kobayashi et al., 2014; Rebsamen et al., 2015; Bröer et al., 2016; Chan et al., 2016; Dong et al., 2018) were still present at normal levels (Fig. 6 B), suggesting that it is likely not the influx of amino acids that is perturbed in the retromer-deficient U2OS cells. By costaining of the retromer component SNX1 and endogenous mTOR, we also analyzed whether retromer and mTOR colocalize on endosomal compartments. While confocal analysis of SNX1 and mTOR suggested some colocalization on vesicular compartments (Fig. 6 C), a 3D reconstruction of several Z-planes revealed that SNX1 and mTOR are largely separated on endocytic compartments (Fig. 6 D), indicative of an indirect role for retromer in mTORC1 activation. In agreement with the lack of colocalization, we failed to detect binding of overexpressed retromer subunits

with RAPTOR, mLST8, RICTOR, and mTOR. The retromer-associated protein SNX27 precipitated RICTOR and some RAPTOR (Fig. 6 E), but, unlike reported previously (Yang et al., 2018), knockdown of SNX27 did not result in any loss of mTORC1 signaling upon amino acid stimulation (Fig. 6 F), confirming our KO data (Fig. S3 C) that retromer does not regulate mTORC1 through SNX27. We concluded that retromer likely regulates mTORC1 in an indirect manner.

mTORC1 signaling requires regulation of RAB7 activity through retromer/TBC1D5
To investigate the mechanism through which retromer promotes amino acid sensing and mTORC1 signaling, we next performed a CRISPR/Cas9 screen of retromer-associated proteins
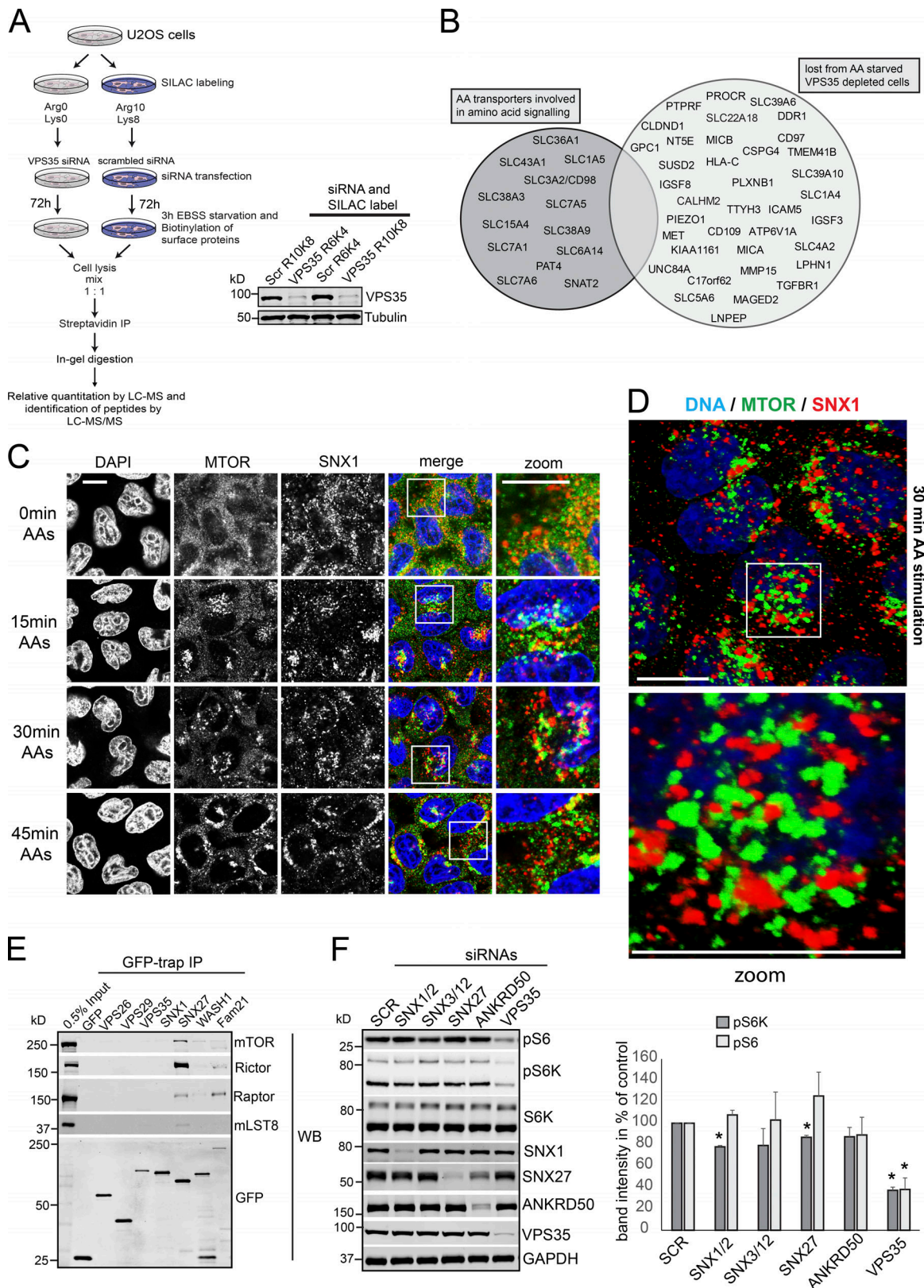
Figure 6. **Retromer does not interact with mTORC1 and does not maintain surface levels of critical amino acid transporters. (A)** Schematic representation of the SILAC work flow to quantify the cell surface proteome of VPS35-depleted U2OS cells by LC-MS/MS. Western blotting was used to confirm the efficient depletion of VPS35 in the SILAC-labeled cells. **(B)** Venn diagram showing the overlap between detected amino acid transporters that have been implicated in mTORC1 activation and transmembrane proteins that were lost ≥1.4-fold (average of two experiments) from the surface of VPS35-depleted cells. **(C)** U2OS cells were starved in EBSS for 3 h and stimulated with amino acids for the indicated times, followed by fixation and staining of endogenous mTOR

(Alexa Fluor 488, green) and the retromer component SNX1 (Alexa Fluor 594, red). Confocal microscopy was used to analyze potential colocalization between retromer and mTOR. **(D)** 3D reconstruction of a z-stack of endogenous SNX1 (red) and endogenous mTOR (green). **(E)** GFP-tagged retromer components and retromer-associated proteins were transfected into HEK293 cells and precipitated by GFP-trap, and precipitates were analyzed for the presence of the indicated mTORC1/2 components. **(F)** The indicated retromer components and retromer-associated proteins were depleted with siRNA in U2OS cells, and mTORC1 activity after 45 min of amino acid stimulation was tested through Western blotting of S6K1 and S6 phosphorylation in three independent experiments. Error bars = SD. Scale bars represent 10 μm; *, P < 0.05 in a two-tailed, unpaired t test between the indicated condition and parental/nontreated control cells.

and tested whether genomic deletion of any of them phenocopied the loss of amino acid–mediated mTORC1 substrate phosphorylation. To do so, three plasmids expressing distinct gRNAs targeting different exons of the respective gene were pooled together with a puromycin selection marker. Following puromycin selection of transfected cells and 5-d recovery, cells were starved in medium without serum and amino acids and acutely stimulated with a mixture of amino acids. We included the HOPS (homotypic fusion and protein sorting) complex component VPS39, the loss of which has been shown to disrupt amino acid signaling (Flinn et al., 2010), as a positive control. Besides loss of VPS39 and loss of core retromer component VPS29, only KO of TBC1D5 resulted in a comparable reduction in mTORC1 substrate phosphorylation to loss of VPS29 (Fig. 7 A). TBC1D5 is a retromer-associated RAB7 GAP protein that controls retromer activity and has roles in autophagy (Seaman et al., 2009; Popovic and Dikic, 2014; Roy et al., 2017). Western blotting confirmed the loss of TBC1D5 from the CRISPR-treated cells. We next aimed to investigate the role of TBC1D5 in mTORC1 activation in more detail. Acute KO of TBC1D5 from HeLa cells broadly reduced mTORC1 substrate phosphorylation upon stimulation with amino acids (Fig. 7 B). This was specific for TBC1D5, as KO of TBC1D2 and TBC1D15, two other proteins with reported RAB7 GAP activity (Zhang et al., 2005; Frasa et al., 2010), did not cause comparable mTORC1 activation defects (Fig. 7 C). TBC1D5 requires the direct binding to the retromer component VPS29 for its endosomal localization and for its GAP activity (Jia et al., 2016; Jimenez-Orgaz et al., 2018). Therefore, we next tested whether TBC1D5 needs to bind to retromer to regulate mTORC1 activation. Indeed, mTORC1 substrate phosphorylation could be rescued through lentiviral reexpression of WT GFP-TBC1D5, whereas reexpression of a retromer binding–deficient TBC1D5 mutant (Jia et al., 2016) failed to rescue (Fig. 7 D), indicating that TBC1D5 needs to engage retromer to enable mTORC1 activation. Conversely, a VPS29 mutant (VPS29-L152E) that cannot bind TBC1D5 (Harbour et al., 2010; Hesketh et al., 2014; Jia et al., 2016) failed to rescue mTORC1 activation and lysosomal recruitment in amino acid–stimulated cells, whereas WT VPS29 did so efficiently (Fig. 7, E and F; and Fig. S4 B). Taken together, these data suggested that retromer engages TBC1D5 to regulate mTORC1 activation through amino acids.

## Hyperactivated RAB7a blocks mTORC1 activation

We and others have recently shown that retromer, together with TBC1D5, acts as a master regulator of RAB7 activity and localization (Jimenez-Orgaz et al., 2018; Seaman et al., 2018). In the absence of retromer or TBC1D5, RAB7 is essentially locked into its active state and accumulates on the lysosomal membrane due to decreased nucleotide cycling and membrane turnover. Based

on this, we hypothesized that hyperactivated RAB7 may be the cause of the apparent mTORC1 activation defects. In agreement with this notion, a constitutively active RAB7 variant has previously been reported to be a potent inhibitor of amino acid–mediated mTORC1 activation (Li et al., 2010). We confirmed this data and found that low-level overexpression (roughly the same level as endogenous RAB7) of constitutively active RAB7-Q67L disrupted amino acid–mediated mTORC1 substrate phosphorylation (Fig. S4 A). If hyperactive RAB7 caused the mTORC1 phenotype in retromer-deficient cells, down-regulation of RAB7 activity should at least partially restore mTORC1 activity. To test this, we next infected the VPS29 KO cells with a lentivirus encoding dominant-negative RAB7 (GFP-RAB7-T22N), which should down-regulate or block endogenous RAB7 activity. Indeed, expression of RAB7-T22N, but not WT GFP-RAB7, efficiently restored amino acid–mediated phosphorylation of the mTORC1 substrate S6K (Fig. 8 A), confirming that it is indeed hyperactivated RAB7 that perturbs mTORC1 signaling upon loss of retromer. CRISPR/Cas9-mediated targeting of endogenous CCZ1, which, together with MON1, is the main RAB7-activating protein (Nordmann et al., 2010; Gerondopoulos et al., 2012), also restored mTORC1 activity in a VPS29 KO background (Fig. 8 B). KO as well as knockdown of endogenous RAB7a partially rescued mTORC1 signaling in VPS29 KOs (Fig. 8, C and D), thereby demonstrating that the hyperactivated, endogenous RAB7a is responsible for a large part of the mTORC1 defects observed upon loss of retromer.

RAB7 aberrantly enters the mTORC1 domain in the absence of retromer

Since RAB proteins establish functional microdomains on endosomal membranes (Pfeffer, 2013), we hypothesized that the hyperactivation of RAB7 may lead to an expansion of this GTPase into the lysosomal domain that senses amino acids, thereby impairing its function. Indeed, a colocalization analysis of GFP-RAB7, expressed at very low levels, and endogenous mTOR indicated that RAB7 and mTOR partially reside on the same endolysosome but localize to largely distinct subdomains (Fig. S4, C and D). A substantial fraction of vesicular mTOR also resided on RAB7-negative vesicular entities in the cell periphery (Fig. S4 C), which have been shown to be the most active sites of mTORC1 signaling (Korolchuk et al., 2011). Constitutively active GFP-RAB7-Q67L was much more vesicular and appeared to displace mTOR from late endosomes/lysosomes, as mTOR did not reside on RAB7-Q67L–decorated vesicles (Fig. S4 D). In contrast, dominant-negative RAB7-T22N did not localize to lysosomes but resulted in increased vesicular localization of mTOR (Fig. S4 D). Costaining of endogenous RAB7 and the lysosome marker LAMP2 in parental and VPS35 KO HeLa cells revealed
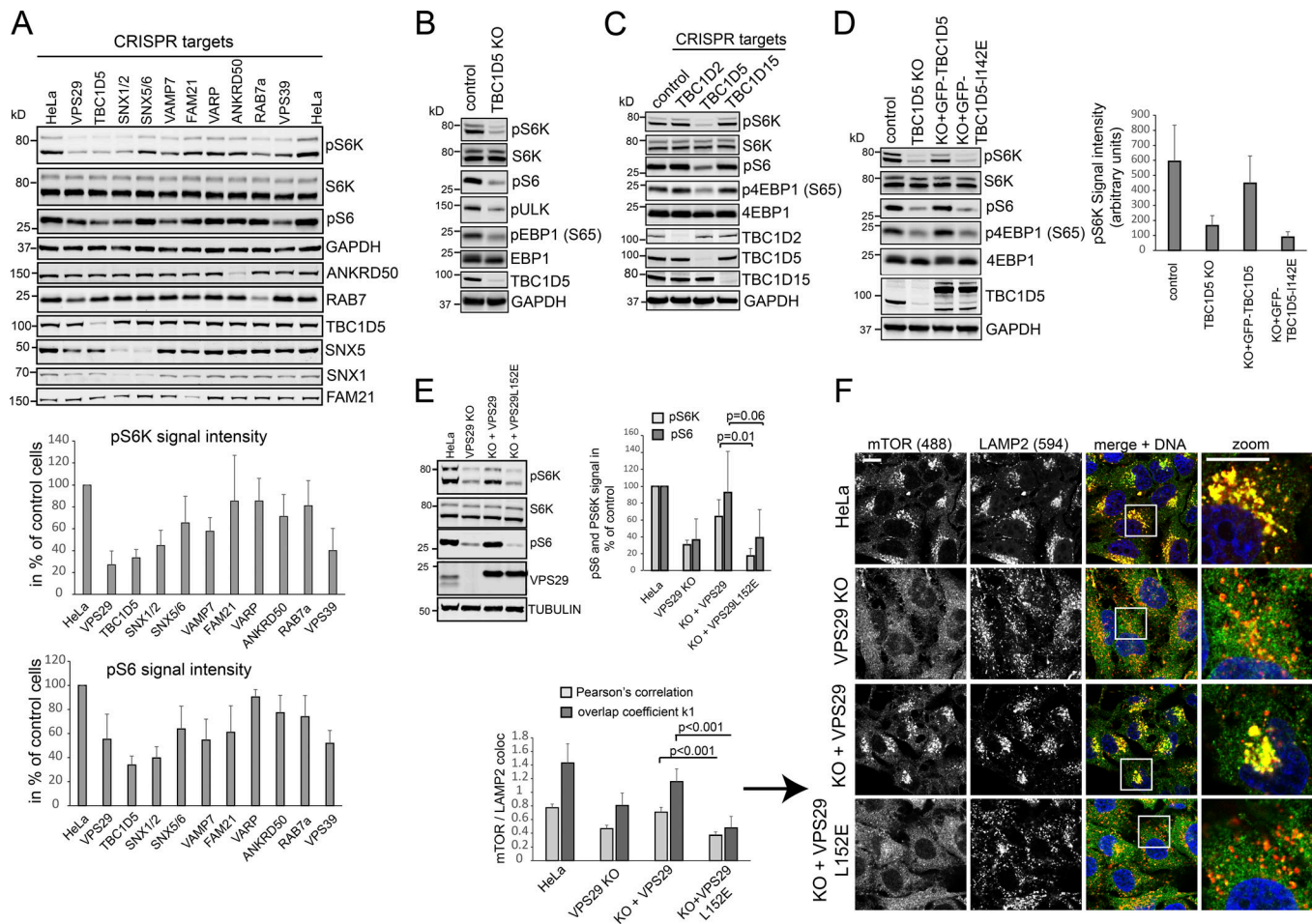
Figure 7. **CRISPR/Cas9 screening identifies TBC1D5 as the retromer component that maintains amino acid signaling. (A)** HeLa cells were transfected with Cas9, a pool of three gRNAs targeting the indicated retromer component, and a puromycin resistance construct. Transfectants were selected with puromycin and incubated for 5 d, followed by starvation in serum- and amino acid–free medium for 3 h and acute (45-min) stimulation with a mixture of amino acids (MEM recipe and glutamine). mTORC1 activity upon amino acid stimulation was assessed by Western blotting of pS6K1 and pS6. The quantification was done across six independent experiments. **(B)** HeLa cells were transfected with a pool of gRNAs targeting the TBC1D5 gene, starved in serum-free DMEM, and stimulated with a mixture of amino acids. mTORC1 substrate phosphorylation was assessed by Western blotting. **(C)** HeLa cells were transfected with a mix of gRNAs targeting the indicated RAB7 GAP proteins. The cells were then starved in serum-free DMEM and stimulated with amino acids for 45 min, and mTORC1 substrate phosphorylation was analyzed by Western blotting. **(D)** HeLa cells were transfected with a mix of gRNAs targeting TBC1D5. 5 d after transfection, the KO cells were infected with a lentivirus encoding GFP-tagged TBC1D5 and the retromer-binding mutant TBC1D5-L142E. The cells were then starved in serum-free DMEM and stimulated with amino acids for 45 min, and mTORC1 substrate phosphorylation was analyzed by Western blotting ($n = 4$). **(E)** Clonal VPS29 KO cells were infected with a lentivirus encoding WT and TBC1D5 binding deficient VPS29-L152E, starved in amino acid–free DMEM, and stimulated with amino acids. mTORC1 substrate phosphorylation was assessed by Western blotting in three independent experiments. **(F)** The cells were treated as in E, fixed, and stained for endogenous mTOR (Alexa Fluor 488, green) and LAMP2 (Alexa Fluor 594, red). Colocalization was quantified across 12 images from two independent experiments. Error bars = SD. Scale bars represent 10 μm; P values stem from a two-tailed, unpaired t test between the indicated conditions.

that the partial and punctate localization of endogenous RAB7 to lysosomes was dramatically altered in the retromer-deficient cells, as RAB7 fully covered the entire LAMP2-decorated domain (Figs. 8 E and S4 E). We observed similar changes for GFP-RAB7, which partially localized to lysosomes in WT cells but fully covered all lysosomes in VPS35-deficient cells (Fig. S4 F). Enhanced-resolution confocal imaging (Airyscan technology) of endogenous LAMTOR1 and GFP-RAB7 expressed at low levels revealed that ragulator and RAB7 resided on well-separated microdomains on LAMP1-stained lysosomes (Fig. 8 F). This separation was reduced markedly in VPS29- and VPS35-deficient cells under the same imaging conditions (Fig. 9 A). The colocalization between GFP-RAB7

and endogenous LAMTOR1 was significantly increased in VPS29- and VPS35-KO cells (Fig. 9 B). This was particularly evident on peripheral lysosomes, which were often LAMTOR1 positive but RAB7 negative (Fig. 9 B). Strikingly, the merging of the RAB7 and Ragulator signal could be reverted by reexpression of WT VPS29, whereas the TBC1D5 binding–deficient VPS29-L152E failed to restore the separation between RAB7 and ragulator (Fig. 9 B). RAB7 did not interact with ragulator, RAGs, or mTORC1 components (Fig. S5, A–C), indicating that RAB7 does not directly block RAG–ragulator interactions but instead interferes with RAG–ragulator dynamics indirectly. Based on these data, we propose that retromer prevents "leakage" of activated RAB7 into the amino
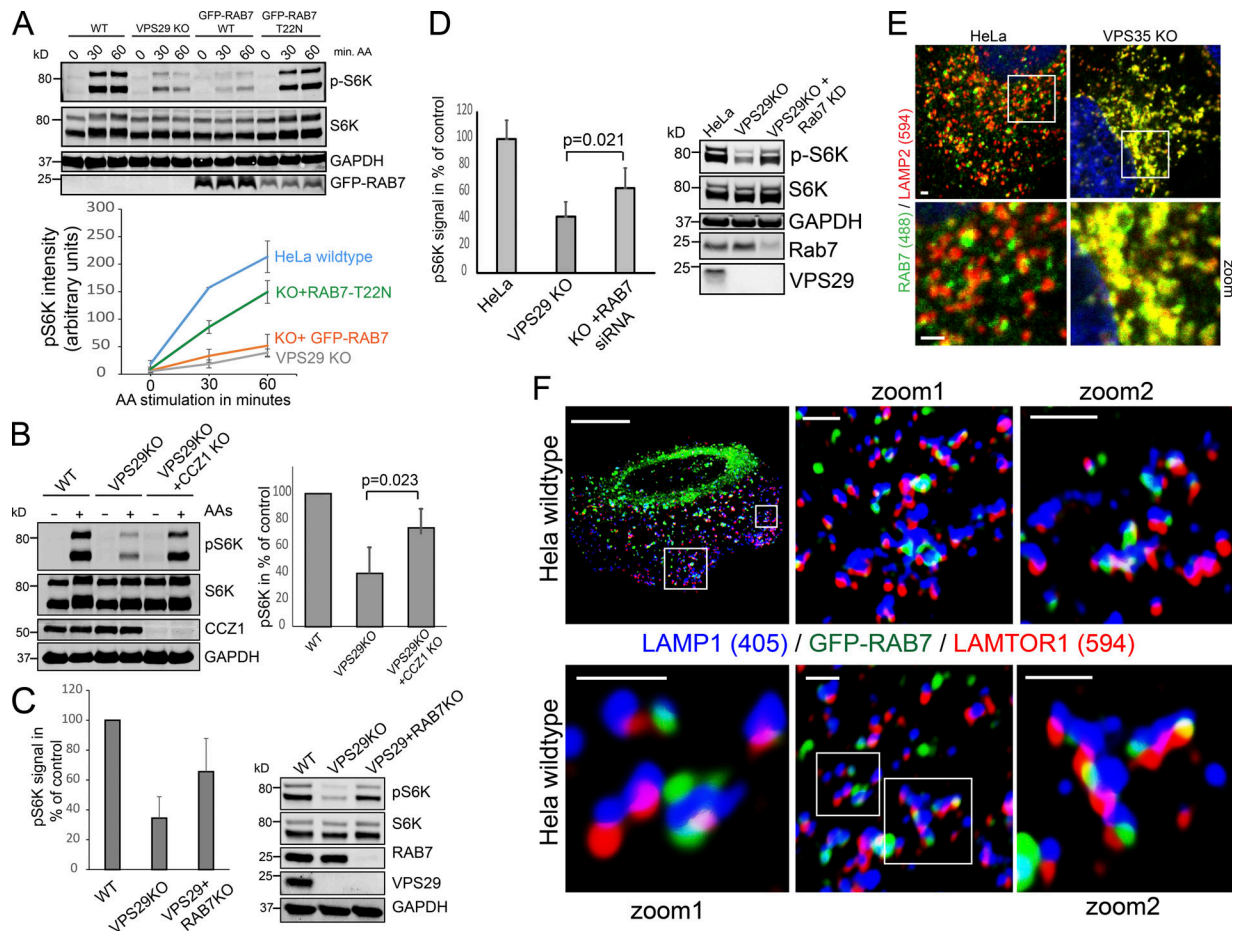
Figure 8. **Hyperactivated RAB7 disrupts amino acid signaling. (A)** Parental HeLa cells, VPS29 KO cells, and VPS29 KOs infected with a lentivirus encoding GFP-RAB7 and dominant-negative GFP-RAB7-T22N were starved in amino acid–free DMEM and stimulated with amino acids for 45 min. The level of phosphorylated S6K1 was then determined and quantified by Western blotting over three independent experiments. **(B)** Parental HeLa cells, VPS29 KO cells, and VPS29 KO cells transfected with Cas9 and a pool of three gRNAs against the RAB7-activating GEF protein CCZ1 were starved in amino acid–free DMEM and stimulated with amino acids for 45 min. The level of phosphorylated S6K1 was then determined and quantified by Western blotting over three independent experiments. **(C)** Parental HeLa cells, VPS29 KO cells, and VPS29/RAB7a double-KO cells were starved in amino acid–free DMEM and stimulated with amino acids for 45 min. The level of phosphorylated S6K1 was then determined and quantified by Western blotting over three independent experiments. **(D)** Parental HeLa cells, VPS29 KO cells, and VPS29 KOs treated with siRNA against endogenous RAB7 were starved in amino acid–free DMEM and stimulated with amino acids for 45 min. The level of phosphorylated S6K1 was then determined and quantified by Western blotting over three independent experiments. **(E)** Parental HeLa cells and VPS35 KO cells were fixed and stained for endogenous RAB7 (Alexa Fluor 488, green) and endogenous LAMP2 (Alexa Fluor 594, red). Images were acquired by confocal microscopy. **(F)** HeLa WT cells were infected with a lentivirus expressing GFP-RAB7a at low levels. The cells were then fixed in PFA and stained for endogenous LAMTOR1 (Alexa Fluor 594, red) and LAMP1 (Alexa Fluor 405, blue). Z-stacked images were acquired on a Zeiss confocal microscope equipped with Airyscan detectors to achieve higher resolution. The images display a 3D reconstruction after Airyscan processing. Scale bars represent 1 µm (F). Error bars = SD; P values stem from a two-tailed, unpaired *t* test between the indicated conditions.

acid–sensing domain by deactivating this small GTPase on maturing endosomes.

Finally, we aimed to investigate whether loss of retromer would affect mTORC1 activity in a more physiologically relevant setting. For this, we tested whether RNAi-mediated depletion of VPS29 or VPS35 in *Caenorhabditis elegans* would increase the lifespan of worms, as would be expected with reduced mTORC1 activity (Templeman and Murphy, 2018). Western blotting of an exogenous reporter construct based on the human mTORC1 substrate 4E-BP1 confirmed that mTORC1-mediated phosphorylation of this reporter was reduced in VPS29- and VPS35-suppressed worms (Fig. 9 C), indicating a loss of mTORC1 signaling. Strikingly, knockdown

of VPS29 or VPS35 increased the lifespan of the worms, similar to the increase observed with knockdown of mTORC1 component *daf-15* (RAPTOR homologue), suggesting that retromer also regulates mTORC1 in living nematodes (Fig. 9 D). This increase in lifespan was most likely due to reduced mTORC1 activity, as the GFP tagged TFEB homologue *hlh-30*, which is maintained in the cytosol through mTORC1 activity (Lapierre et al., 2013), robustly translocated to the nucleus of intestinal cells in worms treated with VPS29 or VPS35 RNAi (Fig. 9 E). Finally, we asked whether RAB7 may also be a regulator of mTORC1 signaling independently of retromer. Indeed, knockdown of RAB7 resulted in a measurable increase in amino acid–mediated mTORC1 activation, as indicated
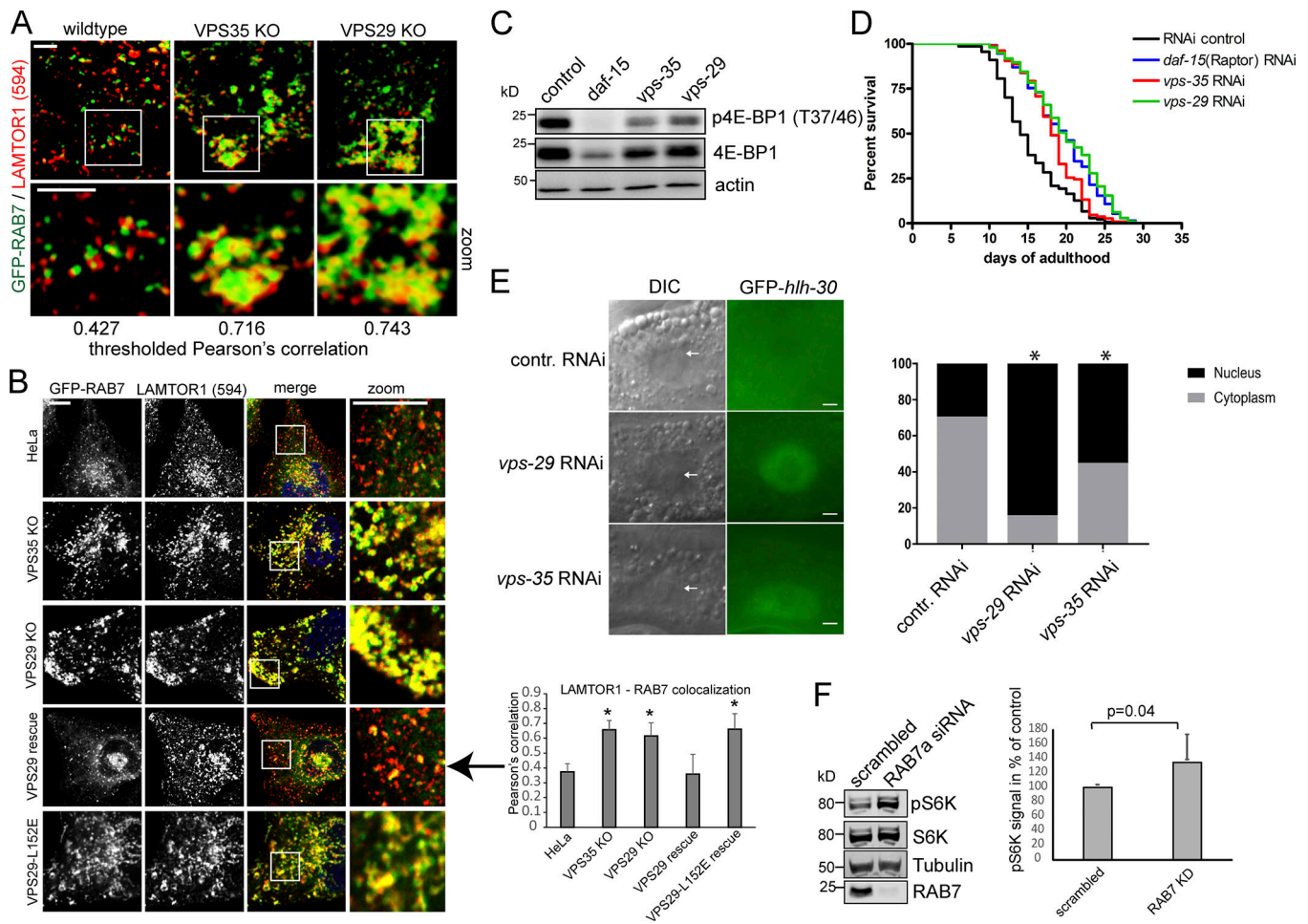
Figure 9. **Loss of retromer causes expansion of RAB7a into the ragulator domain and increases lifespan in *C. elegans*. (A)** The indicated HeLa cell lines expressing lentiviral GFP-RAB7a were stained for endogenous LAMTOR1 (Alexa Fluor 594, red). Z-stacks were acquired on a confocal microscope with Airyscan detector technology. The images show 3D reconstructions of the Z-stacks following Airyscan processing. **(B)** Parental HeLa cells, VPS35 KO cells, VPS29 KO cells, and VPS29 KO cells with lentiviral reexpression of VPS29 and the TBC1D5 binding–deficient VPS29-L152E were infected with a lentivirus encoding GFP-RAB7. The cells were fixed and costained for the ragulator component LAMTOR1 (Alexa Fluor 594, red). The colocalization between GFP-RAB7 and LAMTOR1 was then analyzed by confocal microscopy and quantified across 20 images per condition acquired in two independent experiments. **(C)** *C. elegans* worms were treated with RNAi to suppress the RAPTOR homologue daf-15 and the retromer components vps-35 and vps-29 and tested for mTORC1 activity with an exogenous reporter construct based on phosphorylation of human 4E-BP1 (Western blot panel). **(D)** The RNAi-treated worms described in C were assessed for their lifespan. The number of worms quantified were 134 (control), 106 (vps-35 RNAi), 97 (vps-29 RNAi), and 130 (daf-15). **(E)** *C. elegans* worms expressing the TFEB homologue GFP-hlh-30 were treated with RNAi to suppress the retromer components vps-35 and vps-29, and the nuclear localization of GFP-hlh-30 in intestinal cells was assessed by microscopy. *, P < 0.001 by two-way ANOVA. The quantification was done across a total of 60 worms in three independent experiments. **(F)** HeLa cells were transfected with siRNA against RAB7a, and mTORC1 activity was assessed by Western blotting of phosphorylated S6K1 protein. The quantification was done across four independent experiments. Error bars = SD. Scale bars represent 1 µm (A) or 5 µm (B); P values represent the results of an unpaired, two-tailed *t* test (Excel) between the indicated conditions. *, P < 0.05 in a two-tailed, unpaired *t* test between the indicated condition and parental/nontreated control cells. All P values are from the same type of *t* test.

by increased S6K phosphorylation (Fig. 9 G), suggesting that RAB7 may be an endogenous regulator of mTORC1 signaling.

Discussion

Here, we demonstrate that retromer-mediated control of RAB7 domain architecture is required for late endosomal/lysosomal amino acid sensing and mTORC1 recruitment and signaling. According to our data, retromer promotes mTORC1 signaling in yeast, worms, and mammalian cells. Thus, we propose that retromer should be considered an evolutionarily conserved

upstream component or regulator of the cellular amino acid signaling machinery.

Mechanistically, our data suggest that retromer does not control the cell surface level of critical amino acid transporters in U2OS cells, loss of which from the cell surface could also explain some of the observed defects in amino acid–mediated mTORC1 activation. However, since we have not directly tested amino acid influx into the cells, we cannot rule out that a fraction of the mTORC1 activation defects in retromer null cells is caused by reduced cellular uptake of certain amino acids. Our rescue experiments with the VPS29-L152E mutant that cannot engage TBC1D5 argues that impaired recycling of surface

transporters is unlikely to be the main cause of mTORC1 defects. This mutant fully restores retromer-mediated recycling of cell surface transporters (Jimenez-Orgaz et al., 2018) but completely failed to restore mTORC1 signaling. Thus, we propose that it is not retromer-dependent recycling of cell surface transporters that is required for mTORC1 activity. This also applies to the glucose transporter GLUT1, which we have shown to shuttle glucose into cells in a retromer-dependent manner (Steinberg et al., 2013). The VPS29-L152E mutant fully restores recycling of this critical glucose transporter (Jimenez-Orgaz et al., 2018), so a loss of glucose uptake is unlikely to explain the observed defects in mTORC1 activation.

Instead, our data indicate that the hyperactivated RAB7 GTPase (Jimenez-Orgaz et al., 2018; Seaman et al., 2018) is responsible for a large proportion of the mTORC1 activation defects upon loss of retromer. We have shown previously (Jimenez-Orgaz et al., 2018) and in this study that RAB7 displays a tightly controlled localization to a subset of late endosomes and lysosomes, where it forms discrete patches or microdomains on larger late endosomes. This domain architecture is maintained by retromer and the VPS29-bound TBC1D5, which act cooperatively to deactivate RAB7 on maturing endosomes (Jimenez-Orgaz et al., 2018; Seaman et al., 2018). In the absence of either TBC1D5 or retromer, RAB7 becomes grossly hyperactivated and fully covers the entire late endocytic network. This could be due to either a loss of domain restriction for this small GTPase or simply increased levels of active, membrane-associated RAB7 on late endosomes. We found that endogenous mTOR and the ragulator component LAMTOR1 localize to RAB7-negative late endosomes in the cell periphery as well as to RAB7-positive late endosomes, on which mTOR and RAB7 remain spatially separated. This separation as well as the RAB7-negative lysosome population appear to be completely lost in retromer-deficient cells, so the RAB7 and the ragulator-decorated domain are largely merged. Small GTPases such as the RAB proteins are known to function through microdomains that need to be spatially separated to fulfill their specialized functions (Pfeffer, 2013). Therefore, we propose that the massive presence of RAB7 in the RAG-ragulator domain of retromer-null cells interferes with this functional specification so that ragulator function, and thus amino acid signaling, is impaired. According to recent data (Lawrence et al., 2018), the RAG–ragulator interaction is highly dynamic, and rapid RAG cycling between cytosol and ragulator-decorated domains is required for efficient mTORC1 activation. We propose that the presence of another small GTPase in the ragulator domain interferes with these dynamics, which manifests itself as a loss of the RAG–ragulator interaction, decreased lysosomal RAG levels, and impaired mTORC1 recruitment. Since we could not detect any interaction between RAB7 and RAG, ragulator, or mTORC1 components, we hypothesize that this interference is indirect, probably through a host of effectors that the hyperactivated RAB7 aberrantly recruits to the ragulator domain. The apparent defects in lysosome positioning in our retromer-deficient cells also indicate impaired ragulator function, as ragulator antagonizes the peripheral movement of lysosomes through the recently discovered BORC (biogenesis of lysosome-related organelles complex

1–related complex) and ARL8b (Filipek et al., 2017; Pu et al., 2017). The defect in mTORC1 activation cannot be solely due to impaired RAG activation through the ragulator, as constitutively active RAGA-Q66L did not rescue the defects. It is therefore rather a defect in correct RAG positioning and not necessarily only a defect in RAG activation. Given that the amino acid sensing and mTORC1 recruitment machinery within and on the lysosomal membrane is highly complex and involves correct interplay between the vesicular v-ATPase (Zoncu et al., 2011), the ragulator complex (Sancak et al., 2010), and amino acid channels such as SLC38A9 (Jung et al., 2015; Rebsamen et al., 2015; Wang et al., 2015), it is not entirely surprising that a shift in lysosomal domain architecture would disrupt such a complex functional assembly.

It should be noted here that there must be a redundant or backup mechanism for TBC1D5 in the control of RAB7 activity, as the TBC1D5 KO cells very quickly lost the mTORC1 activation phenotype, within days after CRISPR treatment. Therefore, in this study we used only cells that had been acutely treated with Cas9 and TBC1D5 gRNAs. In contrast, KO of the core retromer resulted in lasting effects that we observed over several months of culture. Thus, the cells can quickly overcome the loss of TBC1D5 but cannot compensate for the loss of retromer. Future studies are required to identify this redundant pathway and also to integrate the role for TBC1D5 in autophagy (Popovic and Dikic, 2014; Roy et al., 2017) with its function in the mTORC1 pathway. TBC1D5 was reported to bind to LC3 and to mediate ATG9a trafficking in a retromer-independent way, thereby promoting autophagy (Popovic and Dikic, 2014). Popovic and Dikic (2014) used shRNA-mediated, stable suppression of TBC1D5, so the mTOR phenotype was likely already compensated. However, they also found a marked increase of lipidated LC3 in stable VPS29-knockdown U2OS cells, supporting our data on enhanced autophagy induction in the absence of retromer.

The block of amino acid signaling through the hyperactivated RAB7 also raises the question of whether RAB7 is also a physiological regulator of mTORC1 signaling. Our data on RAB7 knockdowns in WT cells, which increased mTORC1 output, suggest that RAB7 may indeed be a negative regulator of mTORC1 activity. This intuitively makes sense, as RAB7 is a main mediator of degradative and autophagic processes (Guerra and Bucci, 2016), whereas mTORC1 promotes anabolic processes. Thus, mTORC1 signaling and RAB7 activity could be negatively correlated to maintain homeostasis between degradative and anabolic processes.

Our data establish that retromer is not only a recycling coat complex but instead also serves as a critical regulator of the interface between the early and late endocytic network through tight control of RAB7 localization and activity. Without retromer, late endosomal domain architecture is disrupted, and specialized domains containing the amino acid–sensing machinery are no longer fully operational. Our data on the changes in lysosomal positioning upon starvation in the retromer-deficient cells argue that mTORC1 signaling is not the only late endosomal function that is disrupted upon loss of retromer. It remains to be determined how retromer regulates late endosome/lysosome positioning and thereby parts of the functionality

Kvainickas et al.
Retromer maintains amino acid signaling

Journal of Cell Biology
https://doi.org/10.1083/jcb.201812110

3032

of the late endocytic network. Due to its role in the recycling of lysosomal hydrolase receptors, retromer has historically been linked to lysosomal biogenesis and function, and changes in lysosomal appearance and function have therefore been attributed to a loss of hydrolase delivery (Arighi et al., 2004). Given that the mTORC1–TFEB pathway is an absolutely critical regulator of lysosomal biogenesis (Settembre et al., 2012), our data on the mTORC1 defects in retromer-deficient cells likely warrant a reappraisal of these observations.

Overall, our data identify a critical role for retromer in late endosomal domain architecture and amino acid signaling through mTORC1, thereby establishing a functional link between these two highly conserved complexes. Since mutant retromer causes hereditary Parkinson's disease (Vilariño-Güell et al., 2011; Zimprich et al., 2011), a potential contributing role for deregulated mTORC1 signaling in afflicted neurons remains to be investigated.

Materials and methods

Antibodies
Antibodies used in this study were as follows: from Cell Signaling Technologies, rabbit anti-Akt (9272), rabbit p-Akt (4060), rabbit S6K (2708), rabbit p-S6K (Thr389; 9234), rabbit p-S6 (4858), rabbit Erk1/2 (4695), rabbit p-Erk1/2 (4370), rabbit LAMTOR1 (8975), rabbit Raptor (2280), rabbit Rictor (2114), rabbit mTOR (2983), rabbit TSC2 (4308), rabbit RAGA (4357), rabbit RAGC (5466), rabbit LAMTOR2 (8145), rabbit LAMTOR3 (8168), rabbit LAMTOR4 (13140), rabbit 4EBP1 (9644), rabbit p4EBP1-S65 (9451), rabbit p4EBP1-T37/46 (2855), rabbit p-ULK-S757 (14202), and rabbit NPRL2 (D8K3X); from Abcam, rabbit anti-VPS35 (ab157220), rabbit Rab7 (ab137029), and mouse anti-VPS35 (ab57632); from BD Transduction Laboratories, mouse anti-SNX1 (611482); from Chromotek, rat anti-GFP (3h9); from DSHB, mouse anti-Lamp2 (H4B4-b); from ProteinTech, mouse anti-GAPDH (60004-I-AP) and rabbit anti-TBC1D5 (17078-1-AP); from Sigma-Aldrich, mouse anti-actin (A2228), mouse anti-tubulin (T9026), mouse anti-HA (H9658), and mouse anti-Myc (M4339); from Sigma Prestige, rabbit anti-CCZ1 (HPA045114) and mouse anti-FLAG M2 (F3165); and from Thermo Fisher Scientific, goat anti-VPS29 (PA5-18244).

Western blotting
All the Western blots in this study except the VPS29 blots were acquired with a LI-COR Odyssey SA system to detect fluorescently labeled secondary antibodies (Invitrogen). The respective band intensities were measured using the automatic background subtraction (average top and bottom setting) of the Odyssey software. All quantifications were done across at least three independent experiments as detailed in the figure legends. For the detection of VPS29, a LAS-4000 mini-system (Fujifilm) was used to detect HRP-coupled secondary antibodies.

Yeast strains and growth conditions
Saccharomyces cerevisiae strains used in this study were all derived from BY4741 (MATa *his3Δ1, leu2Δ0, ura3Δ0, met15Δ0* [Brachmann et al., 1998]) and originated from the yeast KO collection (Euroscarf). Yeast strains were made prototrophic by complementing auxotrophic markers with empty vector plasmids and were pregrown in synthetic dropout medium (0.17% yeast nitrogen base, 0.5% ammonium sulfate, 0.2% dropout mix [USBiological], and 2% glucose) to maintain plasmids, centrifuged, and resuspended in synthetic complete medium (synthetic dropout medium with all amino acids, but without ammonium sulfate), starved for amino acids, and then restimulated with 3 mM glutamine.

In vivo TORC1 activity assays
TORC1 activity was assessed as the ratio between the phosphorylation on Thr^{737} of full-length Sch9 (or GFP-Sch9) compared with the total abundance of Sch9 (or GFP-Sch9) using phosphospecific anti-$pThr^{737}$-Sch9 produced by GenScript and anti-Sch9 antibodies (Péli-Gulli et al., 2015).

DNA constructs and mutagenesis
All constructs used in this study were cloned from HeLa cell cDNA and prepared with the Superscript-III kit (Invitrogen), using Kapa HiFi DNA polymerase (KAPABIOSYSTEMS). All site-directed mutagenesis was performed using the Quikchange method (Promega) of fully overlapping primers combined with KAPA HiFi polymerase. The Flag-tagged SLC38A9 was constructed by David Sabatini (Whitehead Institute, Cambridge, MA; Wang et al., 2015). All primer sequences that were used in this study are listed in Table S1.

SILAC-based surface proteomics
For the quantification of the cell surface proteome of VPS35-depleted U2OS cells, the cells were cultured in heavy (Arginine 10 and Lysine 8) and medium-heavy (Arginine 6 and Lysine 4) DMEM for 2 wk. VPS35 was then depleted with siRNA against VPS35 using Dharmafect 1 (Dharmacon). 72 h after transfection, the cells were starved in Earle's balanced salt solution (EBSS) for 3 h to replicate the starvation/stimulation conditions in which we had observed the most pronounced mTORC1 defects (Fig. 3, for example). Following starvation, the cell surface was biotinylated with cleavable sulfosuccinimidyl-20(biotinamido)ethyl-1,3-dithiopropionate (Apex Biotechnology) according to the instructions of the Pierce cell surface biotinylation kit (Thermo Fisher Scientific). After biotinylation, the cells were lysed in TBS, 2% Triton X-100, and Complete Protease Inhibitor cocktail (Roche). Biotinylated proteins were then isolated with Streptavidin Sepharose (GE Healthcare), boiled in mercaptoethanol containing 2× sample buffer, and loaded onto precast SDS-PAGE gels (Invitrogen). The surface proteins were then subjected to in-gel digestion with modified Trypsin (Promega) and quantified by LC-MS/MS on an Orbitrap XL mass spectrometer (Thermo Fisher Scientific). The experiment was repeated once with swapped SILAC labels. Surface proteins that were at least 1.4-fold reduced (average of the two experiments) were regarded as downregulated from the cell surface.

TALEN-mediated VPS35 deletion
The generation of the clones and the respective sequencing to confirm full KOs have been reported previously (Kvainickas

Kvainickas et al.
Retromer maintains amino acid signaling

Journal of Cell Biology 3033
https://doi.org/10.1083/jcb.201812110

et al., 2017a). Briefly, TALEN constructs targeting exon 4 of the human VPS35 gene were purchased from the University of Seoul (Kim et al., 2013) and transfected into U2OS cells using Lipofectamine 2000 (Invitrogen), and clonal cells were isolated using limited dilution. The clones were screened for the loss of VPS35 by Western blotting. Selected clones were then subjected to genomic sequencing of exon 4 and the surrounding region to confirm frame-shifting InDels.

CRISPR/Cas9

To genomically delete protein expression, the px330 plasmid was modified with gene-specific gRNA targeting sequences according to the Zhang laboratory protocol (Cong et al., 2013). The gRNA and Cas9 encoding px330 plasmids were cotransfected with a plasmid encoding N-terminally EGFP-tagged puromycin resistance using Fugene HD (Promega). 24 h after transfection, cells were selected with 3 µg/ml puromycin for 24 h, followed by incubation for 3 d. 5 d after transfection, the cells were used for further experiments or seeded out in 96-well plates (200 µl/well) for clonal selection. The cells were then screened for loss of the respective protein by Western blotting. All targeting sequences were designed with the sgRNA designer of the Broad Institute (http://portals.broadinstitute.org/gpp/public/analysis-tools/sgrna-design). All gRNA sequences are listed in Table S1. For VPS35 and VPS29, clonal cells were isolated. These clones were characterized in detail in a previous study (Kvainickas et al., 2017a).

Cell culture and transfection

HEK-293, U2OS, and HeLa cells were grown in high-glucose DMEM (Gibco) supplemented with 10% (vol/vol) FCS (Sigma-Aldrich) and penicillin-streptomycin (Gibco) and maintained in an incubator at 37°C and 5% CO_2. Cell lines were regularly tested for mycoplasma contamination. For siRNA transfection, Dharmafect-3 (Dharmacon) was used for U2OS cells, while Lipofectamine 2000 (Life Technologies) was used for HeLa cells. All siRNAs were made by Dharmacon or MWG. For DNA transfection, Fugene 6 and Fugene HD (Promega) were used according to the manufacturers' guidelines.

Transduction

To establish stable cell lines, the target DNA was subcloned into the lentiviral vectors pXLG3 or pLVX-puro. The lentiviral constructs, together with psPAX2 (packaging) and pMD2.G (envelope) plasmids (ratio 4:2:1, respectively) were transfected into HEK293 cells using poly-ethylene-imine (Polysciences) in a 1:3 (µg/µg) ratio. 48 h after transfection, the medium containing lentivirus was collected, filtered, and used to infect target cells. If needed, transduced cells were selected with puromycin (3 µg/ml) 24 h after infection. Target protein expression was verified by immunoblotting.

Cell proliferation assay

The cell proliferation rate was assessed by seeding 500 cells in each well of a 96-well plate (Millipore 96 Flat Bottom Transparent Barex), followed by daily measurement of cell numbers with a hexosaminidase-based colorimetric assay (Landegren,

1984). 45 min after adding the hexosaminidase substrate, p-nitrophenol-N-acetyl-fl-D-glucosaminide, to the cells, the amounts of converted substrate were measured using a Tecan Infinite 200 PRO plate reader.

Autophagic flux

U2OS cells stably expressing GFP-LC3 were starved for nutrients in EBSS medium with addition of Bafilomycin A1 (100 nM). Samples were collected at appropriate time points, processed, and analyzed according to standard Western blotting protocol.

Immunoprecipitations by GFP-Trap

The immunoprecipitations with GFP-Trap beads (Chromotek) were performed with both HEK293 and HeLa cells. For HEK293 cells, 20 µg of plasmid DNA containing GFP-tagged bait was transfected into 15-cm dishes using poly-ethylene-imine in a 1:3 (µg/µg) ratio. HeLa cells been transduced with appropriate lentiviral vectors. 48 h after transfection/transduction, cells were lysed in 20 mM Tris-HCl, 50 mM NaCl, 5 mM $MgCl_2$, 0.5% NP-40, and Roche EDTA-free protease inhibitor cocktail. After removing the cell debris, the lysates were incubated for 1 h with GFP trap beads followed by 2× washing in lysis buffer and Western blot–based detection of proteins.

Starvation and stimulation

HeLa cells grown in DMEM (Gibco) were washed twice with PBS and incubated in high-glucose (4 g/ml) serum-free DMEM lacking amino acids (USBiological; D9800-13). U2OS cells were incubated in EBSS medium. After starvation, the amino acid mix (MEM recipe, PAN-Biotech), individual amino acids, or growth factors were added to activate mTOR signaling pathway. The final concentration of amino acids was equivalent to the amino acid concentration in standard DMEM. Cells were harvested after appropriate times and lysed in phosphatase inhibitors (Sigma-Aldrich) containing buffer. The lysates were processed according to standard Western blotting protocol.

Immunofluorescence and confocal microscope image acquisition

For immunofluorescence, cells were fixed with 4% PFA solution in PBS, permeabilized with 0.1% saponin, and blocked with 1% BSA in PBS before applying indicated primary antibodies and corresponding fluorescently labeled secondary antibodies. The fluorochromes used in this study were DAPI and Alexa Fluor 405, 488, and 594 (all from Invitrogen) as indicated in the figures. All microscopy samples were embedded in Mowiol mounting medium. All microscopy images besides the Airyscan enhanced-resolution images were acquired on a Leica SP8 LSM equipped with stimulated emission depletion lasers. The images were acquired at room temperature with a 63× oil-immersion objective (HC PL APO 63×/1.40 Oil CS2, NA 1.4) using the standard Leica Software (LaX) that comes with the microscope. The .LIF files were then opened with Volocity (PerkinElmer), brightness was adjusted evenly across all images and conditions, and the images were exported as bitmap files from Volocity and transferred into Adobe Illustrator via cut and paste from Adobe Photoshop. Where necessary for visibility in the final Illustrator

Kvainickas et al.
Retromer maintains amino acid signaling

Journal of Cell Biology   3034
https://doi.org/10.1083/jcb.201812110

file, brightness was increased uniformly across the entire image and across all conditions shown using Photoshop. Pearson's correlation between the respective channels was quantified with the colocalization tool of Volocity after setting of uniform thresholds across conditions. The colocalization coefficient corresponds to the Mander's coefficient M2 calculated by Volocity after applying uniform thresholds across conditions.

Airyscan enhanced-resolution imaging
The indicated HeLa cells were fixed and stained as described above. Images were acquired on a Zeiss LSM880 confocal microscope equipped with Airyscan detectors at room temperature. The objective was plan-Apochromat, 63×, NA 1.4, oil immersion. Z-stacks were acquired after optimal Airyscan settings had been established for each channel. After acquisition, the stacks were processed by the Airyscan processing feature in Zeiss Zen software. The processed stacks were then opened in Volocity, and 3D images were reconstructed by Volocity. TIFF files were then exported with the view as TIFF feature. For the zoomed images, the zoom tool in Volocity was used, and the zoomed files were again exported as TIFFs and incorporated into the illustrator files.

C. elegans lifespan assay
WT Bristol N2 strain was used for the lifespan assay. As both retromer complex and mTORC1 play important roles in larval development, *daf-15*, *vps-29*, and *vps-35* RNAi knockdown was initiated at day 1 of adult stage via feeding RNAi-expressing HT115 bacteria. The lifespan assay was performed at 20°C, and animals were transferred every day onto new plates during the reproductive period. Animals that died due to bagging of larvae and extrusion of the intestine were censored.

Examination of h4E-BP phosphorylation in C. elegans
20 Is[Pges-1::Flag-h4E-BP1] transgene (ENH441) day 1 adults were collected in Laemmli buffer containing 2% SDS, 10% glycerol, 5% 2-mercaptoethanol, 0.002% bromophenol blue, and 0.063 M Tris HCl, pH ~6.8, and dissolved by incubation at 95°C for 5 min. The whole lysate was subjected to the following Western blot analysis using anti-FLAG antibody (Sigma-Aldrich) and anti-phospho-4E-BP1 antibody (Cell Signaling).

GFP-hlh-30 localization in C. elegans
Strains
The MAH604 sqls19[Phlh-30:.hlh-30::gfp;rol-6] strain was kindly provided by Malene Hansen (Sanford Burnham Prebys Medical Discovery Institute, La Jolla, CA).

In vivo RNAi experiments
To inactivate *vps-29* and *vps-35* by RNAi, the HT115 (DE3) *E. coli* cells were transformed with the L4440-plasmid, carrying the respective gene fragment. The production of double-strand RNA was induced by adding 1 mM IPTG in the nematode growth medium plates containing carbenicillin. L4 animals were transferred to these RNAi-containing nematode growth medium plates and allowed to produce progeny at 20°C. The second

generation of the progeny grown on RNAi plates were scored for a phenotype.

Microscopy
For analysis of nuclear localization of HLH-30::GFP, animals were mounted on 2% agarose pads in M9 buffer containing 2 mM levamisole and examined using either differential interference contrast or fluorescence microscopy. Images were taken using a Zeiss AxioImager.Z1 Microscope, an AxioCam MRm camera, and AxioVision software Rel.4.6.

Statistical analysis
Statistics were analyzed using Prism 7 (GraphPad). Results are presented as a percentage of worms with cytoplasmic and nuclear localization from the analysis of ≥20 worms, performed in triplicate. Two-way ANOVA was applied to calculate statistical differences. Differences with $P < 0.05$ were accepted as statistically significant. Asterisks denote the degree of statistical significance: *, $P < 0.05$; **, $P < 0.01$; and ***, $P < 0.0001$.

Statistical analysis
The results from quantitative Western blotting and quantitative colocalization analysis were analyzed for statistical significance with the Excel *t* test tool (two-tailed, unpaired, two-sample, unequal variance settings). Data distribution was assumed to be normal, but this was not formally tested. The number of samples, images, or experiments is indicated in the respective figure legends.

Online supplemental material
Fig. S1 shows additional data on the clonal retromer-deficient cell lines. Fig. S2 shows analysis of growth factor and amino acid signaling in retromer-deficient cells. Fig. S3 shows additional data on amino acid signaling in retromer-deficient cells. Fig. S4 shows that hyperactivated RAB7a antagonizes lysosomal mTORC1 recruitment and signaling. Fig. S5 shows that RAB7 does not interact with ragulator, RAGs, or mTORC1. Table S1 lists all gRNA, primer, and RNAi sequences.

References

Arighi, C.N., L.M. Hartnell, R.C. Aguilar, C.R. Haft, and J.S. Bonifacino. 2004. Role of the mammalian retromer in sorting of the cation-independent mannose 6-phosphate receptor. *J. Cell Biol.* 165:123–133. https://doi.org/10.1083/jcb.200312055

Bar-Peled, L., L.D. Schweitzer, R. Zoncu, and D.M. Sabatini. 2012. Ragulator is a GEF for the rag GTPases that signal amino acid levels to mTORC1. *Cell.* 150:1196–1208. https://doi.org/10.1016/j.cell.2012.07.032

Bar-Peled, L., L. Chantranupong, A.D. Cherniack, W.W. Chen, K.A. Ottina, B.C. Grabiner, E.D. Spear, S.L. Carter, M. Meyerson, and D.M. Sabatini. 2013. A Tumor suppressor complex with GAP activity for the Rag GTPases that signal amino acid sufficiency to mTORC1. *Science.* 340:1100–1106. https://doi.org/10.1126/science.1232044

Brachmann, C.B., A. Davies, G.J. Cost, E. Caputo, J. Li, P. Hieter, and J.D. Boeke. 1998. Designer deletion strains derived from *Saccharomyces cerevisiae* S288C: a useful set of strains and plasmids for PCR-mediated gene disruption and other applications. *Yeast.* 14:115–132. https://doi.org/10.1002/(SICI)1097-0061(19980130)14:2<115::AID-YEA204>3.0.CO;2-2

Braschi, E., V. Goyon, R. Zunino, A. Mohanty, L. Xu, and H.M. McBride. 2010. Vps35 mediates vesicle transport between the mitochondria and peroxisomes. *Curr. Biol.* 20:1310–1315. https://doi.org/10.1016/j.cub.2010.05.066

Bröer, A., F. Rahimi, and S. Bröer. 2016. Deletion of Amino Acid Transporter ASCT2 (SLC1A5) Reveals an Essential Role for Transporters SNAT1 (SLC38A1) and SNAT2 (SLC38A2) to Sustain Glutaminolysis in Cancer Cells. *J. Biol. Chem.* 291:13194–13205. https://doi.org/10.1074/jbc.M115.700534

Burd, C., and P.J. Cullen. 2014. Retromer: a master conductor of endosome sorting. *Cold Spring Harb. Perspect. Biol.* 6:a016774. https://doi.org/10.1101/cshperspect.a016774

Chan, K., S.M. Busque, M. Sailer, C. Stoeger, S. Broer, H. Daniel, I. Rubio-Aliaga, and C.A. Wagner. 2016. Loss of function mutation of the Slc38a3 glutamine transporter reveals its critical role for amino acid metabolism in liver, brain and kidney. *Pflugers Arch.* 468:213–227.

Cong, L., F.A. Ran, D. Cox, S. Lin, R. Barretto, N. Habib, P.D. Hsu, X. Wu, W. Jiang, L.A. Marraffini, and F. Zhang. 2013. Multiplex genome engineering using CRISPR/Cas systems. *Science.* 339:819–823. https://doi.org/10.1126/science.1231143

Cui, Y., J.M. Carosi, Z. Yang, N. Ariotti, M.C. Kerr, R.G. Parton, T.J. Sargeant, and R.D. Teasdale. 2019. Retromer has a selective function in cargo sorting via endosome transport carriers. *J. Cell Biol.* 218:615–631. https://doi.org/10.1083/jcb.201806153

Demetriades, C., M. Plescher, and A.A. Teleman. 2016. Lysosomal recruitment of TSC2 is a universal response to cellular stress. *Nat. Commun.* 7:10662. https://doi.org/10.1038/ncomms10662

Derivery, E., C. Sousa, J.J. Gautier, B. Lombard, D. Loew, and A. Gautreau. 2009. The Arp2/3 activator WASH controls the fission of endosomes through a large multiprotein complex. *Dev. Cell.* 17:712–723. https://doi.org/10.1016/j.devcel.2009.09.010

Dong, X., Z. Zhou, B. Saremi, A. Helmbrecht, Z. Wang, and J.J. Loor. 2018. Varying the ratio of Lys:Met while maintaining the ratios of Thr:Phe, Lys:Thr, Lys:His, and Lys:Val alters mammary cellular metabolites, mammalian target of rapamycin signaling, and gene transcription. *J. Dairy Sci.* 101:1708–1718. https://doi.org/10.3168/jds.2017-13351

Feinstein, T.N., V.L. Wehbi, J.A. Ardura, D.S. Wheeler, S. Ferrandon, T.J. Gardella, and J.P. Vilardaga. 2011. Retromer terminates the generation of cAMP by internalized PTH receptors. *Nat. Chem. Biol.* 7:278–284. https://doi.org/10.1038/nchembio.545

Filipek, P.A., M.E.G. de Araujo, G.F. Vogel, C.H. De Smet, D. Eberharter, M. Rebsamen, E.L. Rudashevskaya, L. Kremser, T. Yordanov, P. Tschaikner, et al. 2017. LAMTOR/Ragulator is a negative regulator of Arl8b- and BORC-dependent late endosomal positioning. *J. Cell Biol.* 216:4199–4215. https://doi.org/10.1083/jcb.201703061

Flinn, R.J., Y. Yan, S. Goswami, P.J. Parker, and J.M. Backer. 2010. The late endosome is essential for mTORC1 signaling. *Mol. Biol. Cell.* 21:833–841. https://doi.org/10.1091/mbc.e09-09-0756

Frasa, M.A.M., F.C. Maximiano, K. Smolarczyk, R.E. Francis, M.E. Betson, E. Lozano, J. Goldenring, M.C. Seabra, A. Rak, M.R. Ahmadian, and V.M.M. Braga. 2010. Armus is a Rac1 effector that inactivates Rab7 and regulates E-cadherin degradation. *Curr. Biol.* 20:198–208. https://doi.org/10.1016/j.cub.2009.12.053

Gallon, M., and P.J. Cullen. 2015. Retromer and sorting nexins in endosomal sorting. *Biochem. Soc. Trans.* 43:33–47. https://doi.org/10.1042/BST20140290

Garami, A., F.J.T. Zwartkruis, T. Nobukuni, M. Joaquin, M. Roccio, H. Stocker, S.C. Kozma, E. Hafen, J.L. Bos, and G. Thomas. 2003. Insulin activation of Rheb, a mediator of mTOR/S6K/4E-BP signaling, is inhibited by TSC1 and 2. *Mol. Cell.* 11:1457–1466. https://doi.org/10.1016/S1097-2765(03)00220-X

Gerondopoulos, A., L. Langemeyer, J.R. Liang, A. Linford, and F.A. Barr. 2012. BLOC-3 mutated in Hermansky-Pudlak syndrome is a Rab32/38 guanine nucleotide exchange factor. *Curr. Biol.* 22:2135–2139. https://doi.org/10.1016/j.cub.2012.09.020

Gomez, T.S., and D.D. Billadeau. 2009. A FAM21-containing WASH complex regulates retromer-dependent sorting. *Dev. Cell.* 17:699–711. https://doi.org/10.1016/j.devcel.2009.09.009

Guerra, F., and C. Bucci. 2016. Multiple Roles of the Small GTPase Rab7. *Cells.* 5:34.

Hara, K., Y. Maruki, X. Long, K. Yoshino, N. Oshiro, S. Hidayat, C. Tokunaga, J. Avruch, and K. Yonezawa. 2002. Raptor, a binding partner of target of rapamycin (TOR), mediates TOR action. *Cell.* 110:177–189. https://doi.org/10.1016/S0092-8674(02)00833-4

Harbour, M.E., S.Y.A. Breusegem, R. Antrobus, C. Freeman, E. Reid, and M.N.J. Seaman. 2010. The cargo-selective retromer complex is a recruiting hub for protein complexes that regulate endosomal tubule dynamics. *J. Cell Sci.* 123:3703–3717. https://doi.org/10.1242/jcs.071472

Harbour, M.E., S.Y. Breusegem, and M.N.J. Seaman. 2012. Recruitment of the endosomal WASH complex is mediated by the extended 'tail' of Fam21 binding to the retromer protein Vps35. *Biochem. J.* 442:209–220. https://doi.org/10.1042/BJ20111761

Harrison, M.S., C.S. Hung, T.T. Liu, R. Christiano, T.C. Walther, and C.G. Burd. 2014. A mechanism for retromer endosomal coat complex assembly with cargo. *Proc. Natl. Acad. Sci. USA.* 111:267–272. https://doi.org/10.1073/pnas.1316482111

Helfer, E., M.E. Harbour, V. Henriot, G. Lakisic, C. Sousa-Blin, L. Volceanov, M.N.J. Seaman, and A. Gautreau. 2013. Endosomal recruitment of the WASH complex: active sequences and mutations impairing interaction with the retromer. *Biol. Cell.* 105:191–207. https://doi.org/10.1111/boc.201200038

Hesketh, G.G., I. Pérez-Dorado, L.P. Jackson, L. Wartosch, I.B. Schäfer, S.R. Gray, A.J. McCoy, O.B. Zeldin, E.F. Garman, M.E. Harbour, et al. 2014. VARP is recruited on to endosomes by direct interaction with retromer, where together they function in export to the cell surface. *Dev. Cell.* 29:591–606. https://doi.org/10.1016/j.devcel.2014.04.010

Heublein, S., S. Kazi, M.H. Ogmundsdóttir, E.V. Attwood, S. Kala, C.A.R. Boyd, C. Wilson, and D.C.I. Goberdhan. 2010. Proton-assisted amino-acid transporters are conserved regulators of proliferation and amino-acid-dependent mTORC1 activation. *Oncogene.* 29:4068–4079. https://doi.org/10.1038/onc.2010.177

Inoki, K., Y. Li, T. Xu, and K.L. Guan. 2003. Rheb GTPase is a direct target of TSC2 GAP activity and regulates mTOR signaling. *Genes Dev.* 17:1829–1834. https://doi.org/10.1101/gad.1110003

Jacinto, E., R. Loewith, A. Schmidt, S. Lin, M.A. Rüegg, A. Hall, and M.N. Hall. 2004. Mammalian TOR complex 2 controls the actin cytoskeleton and is rapamycin insensitive. *Nat. Cell Biol.* 6:1122–1128. https://doi.org/10.1038/ncb1183

Jia, D., J.S. Zhang, F. Li, J. Wang, Z. Deng, M.A. White, D.G. Osborne, C. Phillips-Krawczak, T.S. Gomez, H. Li, et al. 2016. Structural and mechanistic insights into regulation of the retromer coat by TBC1d5. *Nat. Commun.* 7:13305. https://doi.org/10.1038/ncomms13305

Jimenez-Orgaz, A., A. Kvainickas, H. Nägele, J. Denner, S. Eimer, J. Dengjel, and F. Steinberg. 2018. Control of RAB7 activity and localization through the retromer-TBC1D5 complex enables RAB7-dependent mitophagy. *EMBO J.* 37:235–254. https://doi.org/10.15252/embj.201797128

Jung, J., H.M. Genau, and C. Behrends. 2015. Amino Acid-Dependent mTORC1 Regulation by the Lysosomal Membrane Protein SLC38A9. *Mol. Cell. Biol.* 35:2479–2494. https://doi.org/10.1128/MCB.00125-15

Karunakaran, S., S. Ramachandran, V. Coothankandaswamy, S. Elangovan, E. Babu, S. Periyasamy-Thandavan, A. Gurav, J.P. Gnanaprakasam, N. Singh, P.V. Schoenlein, et al. 2011. SLC6A14 (ATB0,+) protein, a highly concentrative and broad specific amino acid transporter, is a novel and effective drug target for treatment of estrogen receptor-positive breast cancer. *J. Biol. Chem.* 286:31830–31838. https://doi.org/10.1074/jbc.M111.229518

Kim, D.H., D.D. Sarbassov, S.M. Ali, J.E. King, R.R. Latek, H. Erdjument-Bromage, P. Tempst, and D.M. Sabatini. 2002. mTOR interacts with raptor to form a nutrient-sensitive complex that signals to the cell growth machinery. *Cell.* 110:163–175. https://doi.org/10.1016/S0092-8674(02)00808-5

Kim, D.H., D.D. Sarbassov, S.M. Ali, R.R. Latek, K.V.P. Guntur, H. Erdjument-Bromage, P. Tempst, and D.M. Sabatini. 2003. GbetaL, a positive regulator of the rapamycin-sensitive pathway required for the nutrient-sensitive interaction between raptor and mTOR. *Mol. Cell.* 11:895–904. https://doi.org/10.1016/S1097-2765(03)00114-X

Kim, Y., J. Kweon, A. Kim, J.K. Chon, J.Y. Yoo, H.J. Kim, S. Kim, C. Lee, E. Jeong, E. Chung, et al. 2013. A library of TAL effector nucleases spanning the human genome. *Nat. Biotechnol.* 31:251–258. https://doi.org/10.1038/nbt.2517

Kobayashi, T., S. Shimabukuro-Demoto, R. Yoshida-Sugitani, K. Furuyama-Tanaka, H. Karyu, Y. Sugiura, Y. Shimizu, T. Hosaka, M. Goto, N. Kato, et al. 2014. The histidine transporter SLC15A4 coordinates mTOR-dependent inflammatory responses and pathogenic antibody production. *Immunity.* 41:375–388. https://doi.org/10.1016/j.immuni.2014.08.011

Korolchuk, V.I., S. Saiki, M. Lichtenberg, F.H. Siddiqi, E.A. Roberts, S. Imarisio, L. Jahreiss, S. Sarkar, M. Futter, F.M. Menzies, et al. 2011. Lysosomal positioning coordinates cellular nutrient responses. *Nat. Cell Biol.* 13:453–460. https://doi.org/10.1038/ncb2204

Kvainickas, A., A. Jimenez-Orgaz, H. Nägele, Z. Hu, J. Dengjel, and F. Steinberg. 2017a. Cargo-selective SNX-BAR proteins mediate retromer trimer independent retrograde transport. *J. Cell Biol.* 216:3677–3693. https://doi.org/10.1083/jcb.201702137

Kvainickas, A., A.J. Orgaz, H. Nägele, B. Diedrich, K.J. Heesom, J. Dengjel, P.J. Cullen, and F. Steinberg. 2017b. Retromer- and WASH-dependent sorting of nutrient transporters requires a multivalent interaction network with ANKRD50. *J. Cell Sci.* 130:382–395. https://doi.org/10.1242/jcs.196758

Landegren, U. 1984. Measurement of cell numbers by means of the endogenous enzyme hexosaminidase. Applications to detection of lymphokines and cell surface antigens. *J. Immunol. Methods.* 67:379–388. https://doi.org/10.1016/0022-1759(84)90477-0

Lapierre, L.R., C.D. De Magalhaes Filho, P.R. McQuary, C.C. Chu, O. Visvikis, J.T. Chang, S. Gelino, B. Ong, A.E. Davis, J.E. Irazoqui, et al. 2013. The TFEB orthologue HLH-30 regulates autophagy and modulates longevity in Caenorhabditis elegans. *Nat. Commun.* 4:2267. https://doi.org/10.1038/ncomms3267

Lawrence, R.E., K.F. Cho, R. Rappold, A. Thrun, M. Tofaute, D.J. Kim, O. Moldavski, J.H. Hurley, and R. Zoncu. 2018. A nutrient-induced affinity switch controls mTORC1 activation by its Rag GTPase-Ragulator lysosomal scaffold. *Nat. Cell Biol.* 20:1052–1063. https://doi.org/10.1038/s41556-018-0148-6

Li, L., E. Kim, H. Yuan, K. Inoki, P. Goraksha-Hicks, R.L. Schiesher, T.P. Neufeld, and K.L. Guan. 2010. Regulation of mTORC1 by the Rab and Arf GTPases. *J. Biol. Chem.* 285:19705–19709. https://doi.org/10.1074/jbc.C110.102483

Martina, J.A., Y. Chen, M. Gucek, and R. Puertollano. 2012. MTORC1 functions as a transcriptional regulator of autophagy by preventing nuclear transport of TFEB. *Autophagy.* 8:903–914. https://doi.org/10.4161/auto.19653

McNally, K.E., R. Faulkner, F. Steinberg, M. Gallon, R. Ghai, D. Pim, P. Langton, N. Pearson, C.M. Danson, H. Nägele, et al. 2017. Retriever is a multiprotein complex for retromer-independent endosomal cargo recycling. *Nat. Cell Biol.* 19:1214–1225. https://doi.org/10.1038/ncb3610

Menon, S., C.C. Dibble, G. Talbott, G. Hoxhaj, A.J. Valvezan, H. Takahashi, L.C. Cantley, and B.D. Manning. 2014. Spatial control of the TSC complex integrates insulin and nutrient regulation of mTORC1 at the lysosome. *Cell.* 156:771–785. https://doi.org/10.1016/j.cell.2013.11.049

Nicklin, P., P. Bergman, B. Zhang, E. Triantafellow, H. Wang, B. Nyfeler, H. Yang, M. Hild, C. Kung, C. Wilson, et al. 2009. Bidirectional transport of amino acids regulates mTOR and autophagy. *Cell.* 136:521–534. https://doi.org/10.1016/j.cell.2008.11.044

Nordmann, M., M. Cabrera, A. Perz, C. Bröcker, C. Ostrowicz, S. Engelbrecht-Vandré, and C. Ungermann. 2010. The Mon1-Ccz1 complex is the GEF of the late endosomal Rab7 homolog Ypt7. *Curr. Biol.* 20:1654–1659. https://doi.org/10.1016/j.cub.2010.08.002

Ögmundsdóttir, M.H., S. Heublein, S. Kazi, B. Reynolds, S.M. Visvalingam, M.K. Shaw, and D.C.I. Goberdhan. 2012. Proton-assisted amino acid transporter PAT1 complexes with Rag GTPases and activates TORC1 on late endosomal and lysosomal membranes. *PLoS One.* 7:e36616. https://doi.org/10.1371/journal.pone.0036616

Péli-Gulli, M.P., A. Sardu, N. Panchaud, S. Raucci, and C. De Virgilio. 2015. Amino Acids Stimulate TORC1 through Lst4-Lst7, a GTPase-Activating Protein Complex for the Rag Family GTPase Gtr2. *Cell Reports.* 13:1–7. https://doi.org/10.1016/j.celrep.2015.08.059

Pfeffer, S.R. 2013. Rab GTPase regulation of membrane identity. *Curr. Opin. Cell Biol.* 25:414–419. https://doi.org/10.1016/j.ceb.2013.04.002

Popovic, D., and I. Dikic. 2014. TBC1D5 and the AP2 complex regulate ATG9 trafficking and initiation of autophagy. *EMBO Rep.* 15:392–401. https://doi.org/10.1002/embr.201337995

Pu, J., T. Keren-Kaplan, and J.S. Bonifacino. 2017. A Ragulator-BORC interaction controls lysosome positioning in response to amino acid availability. *J. Cell Biol.* 216:4183–4197. https://doi.org/10.1083/jcb.201703094

Rebsamen, M., L. Pochini, T. Stasyk, M.E.G. de Araújo, M. Galluccio, R.K. Kandasamy, B. Snijder, A. Fauster, E.L. Rudashevskaya, M. Bruckner, et al. 2015. SLC38A9 is a component of the lysosomal amino acid sensing machinery that controls mTORC1. *Nature.* 519:477–481. https://doi.org/10.1038/nature14107

Roczniak-Ferguson, A., C.S. Petit, F. Froehlich, S. Qian, J. Ky, B. Angarola, T.C. Walther, and S.M. Ferguson. 2012. The transcription factor TFEB links mTORC1 signaling to transcriptional control of lysosome homeostasis. *Sci. Signal.* 5:ra42. https://doi.org/10.1126/scisignal.2002790

Rojas, R., T. van Vlijmen, G.A. Mardones, Y. Prabhu, A.L. Rojas, S. Mohammed, A.J.R. Heck, G. Raposo, P. van der Sluijs, and J.S. Bonifacino. 2008. Regulation of retromer recruitment to endosomes by sequential action of Rab5 and Rab7. *J. Cell Biol.* 183:513–526. https://doi.org/10.1083/jcb.200804048

Roy, S., A.M. Leidal, J. Ye, S.M. Ronen, and J. Debnath. 2017. Autophagy-Dependent Shuttling of TBC1D5 Controls Plasma Membrane Translocation of GLUT1 and Glucose Uptake. *Mol. Cell.* 67:84–95.e5. https://doi.org/10.1016/j.molcel.2017.05.020

Sancak, Y., T.R. Peterson, Y.D. Shaul, R.A. Lindquist, C.C. Thoreen, L. Bar-Peled, and D.M. Sabatini. 2008. The Rag GTPases bind raptor and mediate amino acid signaling to mTORC1. *Science.* 320:1496–1501. https://doi.org/10.1126/science.1157535

Sancak, Y., L. Bar-Peled, R. Zoncu, A.L. Markhard, S. Nada, and D.M. Sabatini. 2010. Ragulator-Rag complex targets mTORC1 to the lysosomal surface and is necessary for its activation by amino acids. *Cell.* 141:290–303. https://doi.org/10.1016/j.cell.2010.02.024

Sarbassov, D.D., S.M. Ali, D.H. Kim, D.A. Guertin, R.R. Latek, H. Erdjument-Bromage, P. Tempst, and D.M. Sabatini. 2004. Rictor, a novel binding partner of mTOR, defines a rapamycin-insensitive and raptor-independent pathway that regulates the cytoskeleton. *Curr. Biol.* 14:1296–1302. https://doi.org/10.1016/j.cub.2004.06.054

Sarbassov, D.D., D.A. Guertin, S.M. Ali, and D.M. Sabatini. 2005. Phosphorylation and regulation of Akt/PKB by the rictor-mTOR complex. *Science.* 307:1098–1101. https://doi.org/10.1126/science.1106148

Saxton, R.A., and D.M. Sabatini. 2017. mTOR Signaling in Growth, Metabolism, and Disease. *Cell.* 168:960–976. https://doi.org/10.1016/j.cell.2017.02.004

Seaman, M.N.J. 2004. Cargo-selective endosomal sorting for retrieval to the Golgi requires retromer. *J. Cell Biol.* 165:111–122. https://doi.org/10.1083/jcb.200312034

Seaman, M.N.J., M.E. Harbour, D. Tattersall, E. Read, and N. Bright. 2009. Membrane recruitment of the cargo-selective retromer subcomplex is catalysed by the small GTPase Rab7 and inhibited by the Rab-GAP TBC1D5. *J. Cell Sci.* 122:2371–2382. https://doi.org/10.1242/jcs.048686

Seaman, M.N.J., A.S. Mukadam, and S.Y. Breusegem. 2018. Inhibition of TBC1D5 activates Rab7a and can enhance the function of the retromer cargo-selective complex. *J. Cell Sci.* 131:jcs217398. https://doi.org/10.1242/jcs.217398

Settembre, C., R. Zoncu, D.L. Medina, F. Vetrini, S. Erdin, S. Erdin, T. Huynh, M. Ferron, G. Karsenty, M.C. Vellard, et al. 2012. A lysosome-to-nucleus signalling mechanism senses and regulates the lysosome via mTOR and TFEB. *EMBO J.* 31:1095–1108. https://doi.org/10.1038/emboj.2012.32

Shen, K., and D.M. Sabatini. 2018. Ragulator and SLC38A9 activate the Rag GTPases through noncanonical GEF mechanisms. *Proc. Natl. Acad. Sci. USA.* 115:9545–9550. https://doi.org/10.1073/pnas.1811727115

Steinberg, F., M. Gallon, M. Winfield, E.C. Thomas, A.J. Bell, K.J. Heesom, J.M. Tavaré, and P.J. Cullen. 2013. A global analysis of SNX27-retromer assembly and cargo specificity reveals a function in glucose and metal ion transport. *Nat. Cell Biol.* 15:461–471. https://doi.org/10.1038/ncb2721

Tee, A.R., B.D. Manning, P.P. Roux, L.C. Cantley, and J. Blenis. 2003. Tuberous sclerosis complex gene products, Tuberin and Hamartin, control mTOR signaling by acting as a GTPase-activating protein complex toward Rheb. *Curr. Biol.* 13:1259–1268. https://doi.org/10.1016/S0960-9822(03)00506-2

Temkin, P., B. Lauffer, S. Jäger, P. Cimermancic, N.J. Krogan, and M. von Zastrow. 2011. SNX27 mediates retromer tubule entry and endosome-to-plasma membrane trafficking of signalling receptors. *Nat. Cell Biol.* 13:715–721. https://doi.org/10.1038/ncb2252

Templeman, N.M., and C.T. Murphy. 2018. Regulation of reproduction and longevity by nutrient-sensing pathways. *J. Cell Biol.* 217:93–106. https://doi.org/10.1083/jcb.201707168

Urban, J., A. Soulard, A. Huber, S. Lippman, D. Mukhopadhyay, O. Deloche, V. Wanke, D. Anrather, G. Ammerer, H. Riezman, et al. 2007. Sch9 is a major target of TORC1 in *Saccharomyces cerevisiae*. *Mol. Cell.* 26:663–674. https://doi.org/10.1016/j.molcel.2007.04.020

Vilariño-Güell, C., C. Wider, O.A. Ross, J.C. Dachsel, J.M. Kachergus, S.J. Lincoln, A.I. Soto-Ortolaza, S.A. Cobb, G.J. Wilhoite, J.A. Bacon, et al. 2011. VPS35 mutations in Parkinson disease. *Am. J. Hum. Genet.* 89:162–167. https://doi.org/10.1016/j.ajhg.2011.06.001

Wang, S., Z.Y. Tsun, R.L. Wolfson, K. Shen, G.A. Wyant, M.E. Plovanich, E.D. Yuan, T.D. Jones, L. Chantranupong, W. Comb, et al. 2015. Metabolism. Lysosomal amino acid transporter SLC38A9 signals arginine sufficiency to mTORC1. *Science.* 347:188–194. https://doi.org/10.1126/science.1257132

Wolfson, R.L., and D.M. Sabatini. 2017. The Dawn of the Age of Amino Acid Sensors for the mTORC1 Pathway. *Cell Metab.* 26:301–309. https://doi.org/10.1016/j.cmet.2017.07.001

Xie, M.W., F. Jin, H. Hwang, S. Hwang, V. Anand, M.C. Duncan, and J. Huang. 2005. Insights into TOR function and rapamycin response: chemical genomic profiling by using a high-density cell array method. *Proc. Natl. Acad. Sci. USA.* 102:7215–7220. https://doi.org/10.1073/pnas.0500297102

Yang, Z., J. Follett, M.C. Kerr, T. Clairfeuille, M. Chandra, B.M. Collins, and R.D. Teasdale. 2018. Sorting nexin 27 (SNX27) regulates the trafficking and activity of the glutamine transporter ASCT2. *J. Biol. Chem.* 293: 6802–6811. https://doi.org/10.1074/jbc.RA117.000735

Yu, L., C.K. McPhee, L. Zheng, G.A. Mardones, Y. Rong, J. Peng, N. Mi, Y. Zhao, Z. Liu, F. Wan, et al. 2010. Termination of autophagy and reformation of lysosomes regulated by mTOR. *Nature.* 465:942–946. https://doi.org/10.1038/nature09076

Zavodszky, E., M.N.J. Seaman, K. Moreau, M. Jimenez-Sanchez, S.Y. Breusegem, M.E. Harbour, and D.C. Rubinsztein. 2014. Mutation in VPS35 associated with Parkinson's disease impairs WASH complex association and inhibits autophagy. *Nat. Commun.* 5:3828. https://doi.org/10.1038/ncomms4828

Zhang, X.M., B. Walsh, C.A. Mitchell, and T. Rowe. 2005. TBC domain family, member 15 is a novel mammalian Rab GTPase-activating protein with substrate preference for Rab7. *Biochem. Biophys. Res. Commun.* 335: 154–161. https://doi.org/10.1016/j.bbrc.2005.07.070

Zimprich, A., A. Benet-Pagès, W. Struhal, E. Graf, S.H. Eck, M.N. Offman, D. Haubenberger, S. Spielberger, E.C. Schulte, P. Lichtner, et al. 2011. A mutation in VPS35, encoding a subunit of the retromer complex, causes late-onset Parkinson disease. *Am. J. Hum. Genet.* 89:168–175. https://doi.org/10.1016/j.ajhg.2011.06.008

Zoncu, R., L. Bar-Peled, A. Efeyan, S. Wang, Y. Sancak, and D.M. Sabatini. 2011. mTORC1 senses lysosomal amino acids through an inside-out mechanism that requires the vacuolar H(+)-ATPase. *Science.* 334: 678–683. https://doi.org/10.1126/science.1207056